Article

Cell Host & Microbe

Hemagglutinin Traits Determine Transmission of Avian A/H10N7 Influenza Virus between Mammals

Graphical Abstract

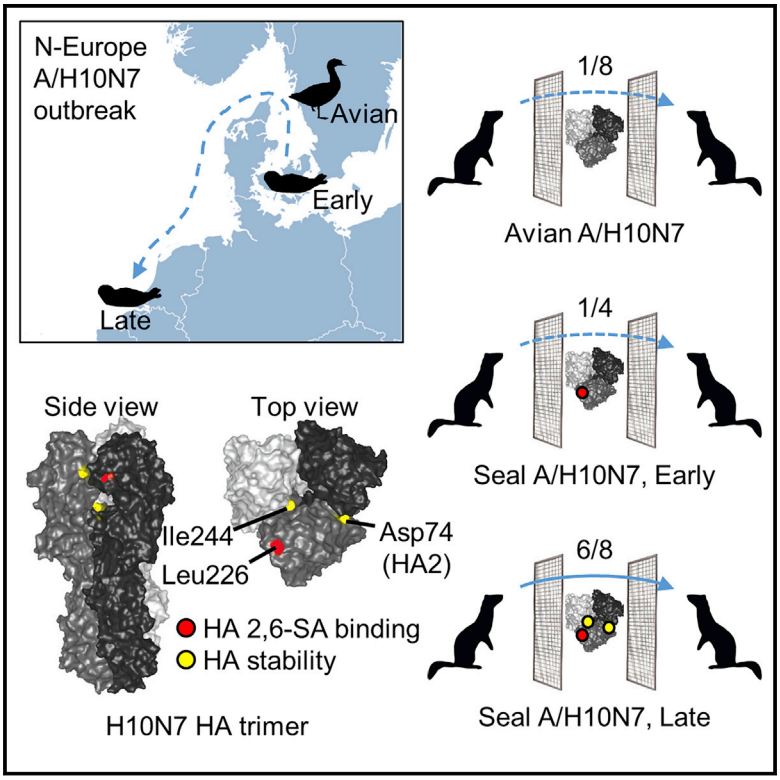

Authors

Sander Herfst, Jie Zhang, Mathilde Richard, ..., James C. Paulson, John J. Skehel, Ron A.M. Fouchier

Correspondence

r.fouchier@erasmusmc.nl

In Brief

Herfst et al. investigated an outbreak in seals caused by an H10N7 influenza virus. In laboratory experiments, this virus was transmissible via the air between ferrets, similar to human influenza viruses. This was caused by mutations that changed the binding pattern and stability of the influenza virus hemagglutinin surface protein.

Highlights

- Adaptation to seals led to transmission of avian A/H10N7 virus between mammals
- Three substitutions in HA altered receptor-binding preference and changed stability
- Receptor-binding specificity substitutions are located in the 220-loop of the HA
- A/H10N7 mammal transmission requirements resemble those for A/H5N1 and other viruses

Herfst et al., 2020, Cell Host & Microbe *28*, 1–12
October 7, 2020
https://doi.org/10.1016/j.chom.2020.08.011

CellPress

Please cite this article in press as: Herfst et al., Hemagglutinin Traits Determine Transmission of Avian A/H10N7 Influenza Virus between Mammals, Cell Host & Microbe (2020), https://doi.org/10.1016/j.chom.2020.08.011

Cell Host & Microbe

CellPress

Article

Hemagglutinin Traits Determine Transmission of Avian A/H10N7 Influenza Virus between Mammals

Sander Herfst,[1,5] Jie Zhang,[2,5] Mathilde Richard,[1] Ryan McBride,[3] Pascal Lexmond,[1] Theo M. Bestebroer,[1] Monique I.J. Spronken,[1] Dennis de Meulder,[1] Judith M. van den Brand,[1,6] Miruna E. Rosu,[1] Stephen R. Martin,[2] Steve J. Gamblin,[2] Xiaoli Xiong,[2] Wenjie Peng,[3] Rogier Bodewes,[1] Erhard van der Vries,[1,7] Albert D.M.E. Osterhaus,[4] James C. Paulson,[3] John J. Skehel,[2] and Ron A.M. Fouchier[1,8,*]

[1]Department of Viroscience, Postgraduate School of Molecular Medicine, Erasmus MC University Medical Center, 3015GE, Rotterdam, the Netherlands

[2]Structural Biology of Disease Processes Laboratory, the Francis Crick Institute, 1 Midland Road, London NW1 1AT, UK

[3]Departments of Molecular Medicine, Immunology and Microbiology, the Scripps Research Institute, La Jolla, CA 92037, USA

[4]Research Centre for Emerging Infections and Zoonoses, University of Veterinary Medicine, 30559, Hannover, Germany

[5]These authors contributed equally

[6]Present address: Department of Pathobiology, Faculty of Veterinary Medicine, Utrecht University, Yalelaan 1, 3581 CL, Utrecht, the Netherlands

[7]Present address: Royal GD, 7418 EZ, Deventer, the Netherlands

[8]Lead Contact

*Correspondence: r.fouchier@erasmusmc.nl

https://doi.org/10.1016/j.chom.2020.08.011

SUMMARY

In 2014, an outbreak of avian A/H10N7 influenza virus occurred among seals along North-European coastal waters, significantly impacting seal populations. Here, we examine the cross-species transmission and mammalian adaptation of this influenza A virus, revealing changes in the hemagglutinin surface protein that increase stability and receptor binding. The seal A/H10N7 virus was aerosol or respiratory droplet transmissible between ferrets. Compared with avian H10 hemagglutinin, seal H10 hemagglutinin showed stronger binding to the human-type sialic acid receptor, with preferential binding to α2,6-linked sialic acids on long extended branches. In X-ray structures, changes in the 220-loop of the receptor-binding pocket caused similar interactions with human receptor as seen for pandemic strains. Two substitutions made seal H10 hemagglutinin more stable than avian H10 hemagglutinin and similar to human hemagglutinin. Consequently, identification of avian-origin influenza viruses across mammals appears critical to detect influenza A viruses posing a major threat to humans and other mammals.

INTRODUCTION

Influenza A viruses are among the most challenging viruses that threaten both human and animal health. In addition to the diversity of host species, influenza A viruses have a remarkable capacity to evolve and adapt after crossing species barriers, to replicate in and transmit between new hosts. The high frequency of inter-species transmission of influenza A viruses results in a high disease burden in humans, pigs, poultry, and to a lesser extent in other mammalian species (Short et al., 2015).

Avian influenza A viruses are classified in subtypes, based on the antigenic and genetic properties of their hemagglutinin (HA) and neuraminidase (NA) membrane glycoproteins. Currently 16 HA subtypes (H1–H16) and 9 NA subtypes (N1–N9) are known to circulate in wild birds, which are the main reservoir of influenza A viruses (Gao, 2018). Influenza A-like viruses of HL17NL10 and HL18NL11 subtypes, identified in bats, have HA- and NA-like proteins substantially different from their homologs in classical avian influenza A viruses (Ma et al., 2015). Occasionally, influenza A viruses from the wild bird reservoir cause sporadic infections, or even outbreaks, in new host species.

In this regard, H10 subtype influenza A viruses from waterfowl have occasionally infected mammals. An A/H10N4 virus caused an outbreak in mink in 1984 (Klingeborn et al., 1985), and an A/H10N5 virus was detected in swine in 2008 (Wang et al., 2012). A/H10N7 viruses were found to cause sporadic human infections in Egypt in 2004 (PAHO, 2004) and in Australia in 2010 (Arzey et al., 2012). More recently, three human cases of infection with A/H10N8 were detected between December 2013 and February 2014 (Chen et al., 2014). These patients, all of whom were isolated cases, were known to have a history of visiting live poultry markets before disease onset, suggesting that poultry were the source of their infections (Zhang et al., 2014).

In spring 2014, avian influenza A/H10N7 virus infections caused an outbreak in harbor seals (*Phoca vitulina*) and gray seals (*Halichoerus grypus*) in North-European coastal waters. Initially, more than 500 dead harbor seals were found off the coasts of western Sweden and eastern Denmark (Krog et al.,

Please cite this article in press as: Herfst et al., Hemagglutinin Traits Determine Transmission of Avian A/H10N7 Influenza Virus between Mammals, Cell Host & Microbe (2020), https://doi.org/10.1016/j.chom.2020.08.011

2015; Zohari et al., 2014), and subsequently the outbreak continued south to seals off the coasts of western Denmark and Germany, resulting in the death of another estimated 1,500–2,000 seals, more than 10% of that seal population (Bodewes et al., 2015). More to the south, in the Netherlands, dozens of seals were found dead toward the end of the outbreak.

Phylogenetic analysis showed amino-acid sequence differences between the HA of seal A/H10N7 viruses and closely related Eurasian avian A/H10N7 viruses and the accumulation of amino-acid substitutions in seal A/H10N7 viruses over time (Bodewes et al., 2016). One of these substitutions was a known mammalian adaptation marker HA Q226L (H3 HA numbering is used throughout the manuscript) in the HA receptor-binding site. Although an avian-origin A/H10N7 virus appeared to have spread efficiently in this new host, neither the transmission route between seals nor the need for adaptation of these avian influenza A viruses to infect and transmit among seals is known. Furthermore, since the known avian-origin A/H10N7 and A/H10N8 viruses have demonstrated their ability to infect humans, it is possible that the avian-origin mammalian-adapted seal A/H10N7 virus poses an even greater risk for humans. To address this concern that the A/H10N7 virus could be sufficiently adapted and able to spread between and among other mammals, potentially including humans, the transmissibility of the seal A/H10N7 virus via aerosols or respiratory droplets was investigated in the ferret model. Following transmission of the seal A/H10N7 virus, it was compared with a closely related avian A/H10N7 virus to determine which properties had changed in the transmissible seal A/H10N7 virus. Since the major phenotypic differences were attributed to HA, the three-dimensional structures of the mutant seal H10 HA's and of the complexes that they form with avian- and human-type receptor analogs were determined. Combined with biolayer interferometry and glycan array analyses, the receptor-binding preference of the aerosol or respiratory droplet-transmissible virus for human sialic acid receptor analogs was demonstrated. Data from membrane fusion assays showed that the seal A/H10N7 HA was acid stable, which was recently demonstrated to be of importance for transmission of highly pathogenic avian influenza (HPAI) A/H5N1 and other viruses via the aerosol or respiratory route. We discuss our observations in the light of an avian H10-seal H10 comparison to better understand the importance of particular changes in HA for transmission between mammals.

RESULTS

Transmission of A/H10N7 Virus via Aerosols or Respiratory Droplets between Ferrets

To study the ability of A/H10N7 viruses to transmit via aerosols or respiratory droplets between ferrets, transmission experiments were performed as described previously (Munster et al., 2009). First, the transmissibility of an A/H10N7 virus that was isolated from a lung sample collected from a seal in Germany in October 2014, A/harbor seal/Germany/1/14 (H10sealG) (Bodewes et al., 2015) was studied. Although the consensus sequence of the H10sealG HA showed an avian-type-receptor-binding signature with a glutamine at position 226 and a glycine at position 228, deep sequence analysis showed that variants typical of human-type-receptor-binding sites were present at both positions, namely Q226L and G228S. In addition, the codon for the residue at position 228 was not found in 13% of the sequence reads of this sample, and this deletion was only present in combination with the Q226L mutation (Bodewes et al., 2015). When H10sealG was tested for transmissibility, one out of four recipient ferrets produced a virus culture-positive throat swab at 5 days post exposure (dpe) (Figures 1 and S1). Serum collected from this animal at 14 dpe had a hemagglutination inhibition (HI) antibody titer of 640, confirming transmission and subsequent replication of H10sealG. When the virus-positive swab from the recipient animal was subjected to sequencing, it turned out that the Q226L substitution was positively selected during transmission via aerosols or respiratory droplets. At the same time, the transmissibility of a recombinant A/harbor seal/Netherlands/PV14-221_TS/2015 (H10sealNL, isolated in January 2015) (Bodewes et al., 2016) was investigated, which already contained a leucine at position 226 and in addition a genetically related avian A/H10N7 virus that was isolated from a mallard in the Netherlands in 2014, A/mallard/NL/1/2014 (H10mall). In these experiments, the H10sealNL virus was transmitted in 6 out of 8 ferret pairs, significantly more than with H10mall that was transmitted in 1 out of 8 transmission pairs (Fisher's exact test, $p = 0.04$) (Figures 1 and S1).

HA Is the Main Determinant of Phenotypic Differences

Previously, three phenotypic changes were described that render A/H5N1 influenza viruses transmissible via aerosols or respiratory droplets between ferrets: binding to the human-type α2,6 sialic acid receptors in the upper respiratory tract, HA acid and temperature stability, and high polymerase activity (Imai et al., 2012; Linster et al., 2014). Because of the genetic differences between the genomes of the mallard and seal influenza viruses (Table S1), the contribution of the viral genes to possible phenotypic differences was studied. Minigenome assays in 293T cells, plaque assays in Madin-Darby canine kidney (MDCK) cells and replication curves in seal kidney cells indicated that there was no difference in activity of the polymerase complexes of the seal and mallard viruses (Figure S2). In addition, an enzyme-linked lectin assay (ELLA) demonstrated that there were no apparent differences in NA activity between the mallard and seal influenza viruses (Figure S2). Given that there was no indication of any other gene contribution, further investigations were focused on the HA protein.

Receptor-Binding Specificity and Avidity of A/H10N7 Viruses

During circulation in seals, the avian-origin A/H10N7 viruses acquired mutations that may have facilitated efficient virus spread in the new host and associated transmissibility in the ferret model. To assess the influence of these mutations on the receptor-binding specificity of the A/H10 HAs, the attachment patterns of A/Puerto Rico/8/1934 (PR8) viruses harboring, H10sealNL, H10mall, or mutant H10 HA proteins were characterized using a custom sialoside glycan array composed of diverse α2,3 (#11–79) and α2,6 (#80–135) sialosides, including extended sialosides that have been observed in human and ferret upper airway tissues (Peng et al., 2017). A/Indonesia/5/05 (A/H5N1) and A/Netherlands/213/03 (A/H3N2) HA served as controls for avian and human specificity respectively (Figures 2A and 2B).

Please cite this article in press as: Herfst et al., Hemagglutinin Traits Determine Transmission of Avian A/H10N7 Influenza Virus between Mammals, Cell Host & Microbe (2020), https://doi.org/10.1016/j.chom.2020.08.011

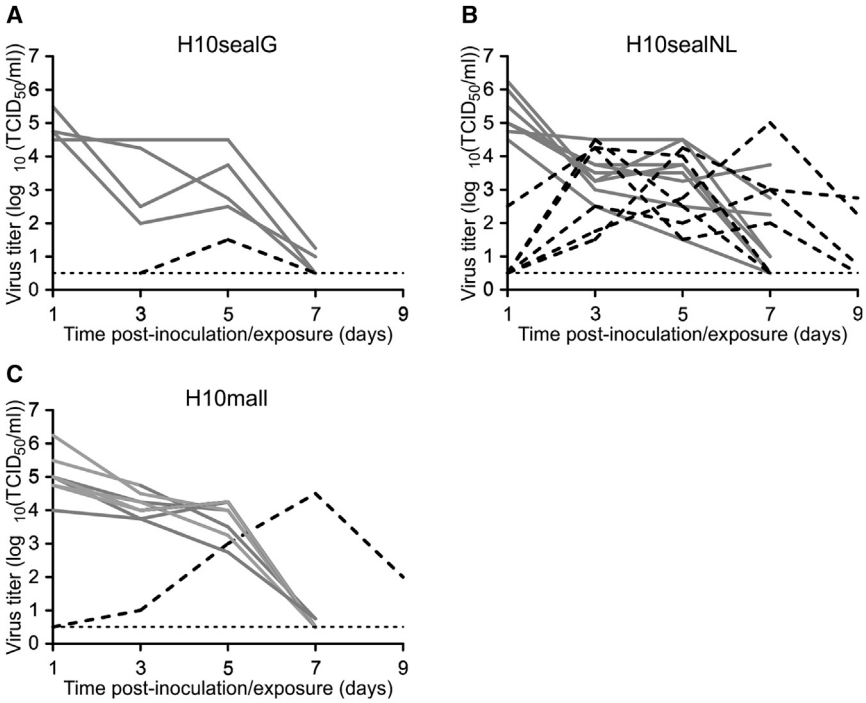

Figure 1. Transmission of A/H10N7 Viruses via Aerosols or Respiratory Droplets between Ferrets

(A–C) Transmission experiments are shown for H10sealG (A), H10sealNL (B), and H10mall (C). Four (A) or eight (B and C) donor ferrets were inoculated intranasally with 10^6 $TCID_{50}$ of virus and housed individually in transmission cages. A naive recipient ferret was added to each transmission cage adjacent to a donor ferret at 1 dpi. Virus titers in throat swabs of donors (gray lines) and recipients (black dashed lines) were determined by end-point titration in MDCK cells. Transmission via aerosols or respiratory droplets was observed in 1 out of 4 ferret pairs for H10sealG, 6 out of 8 ferrets pairs for H10sealNL, and 1 out of 8 ferret pairs for H10mall. The dotted lines indicate the lower limit of virus detection.

H10mall as well as another avian A/H10 HA (A/mallard/Sweden/51/2002 – A/H10N2mall) showed a clear avian-type (α2,3-linked) receptor specificity, although some low binding to α2,6 receptors was observed for H10mall (Figures 2C and 2D). In contrast, H10sealNL showed a mixed specificity for α2,3- and α2,6 receptors, with preferential binding to α2,6 receptors with longer extensions on bi-antennary O-linked glycans (#106–108) and bi- and tri-antennary N-linked glycans (#115–131) (Figure 2E). To assess the role of the HA Q226L substitution on the receptor-binding preference of A/H10 HA, the effect of this substitution in H10mall was analyzed, and the binding preference of the naturally occurring mutants in the receptor-binding site of H10sealG was also studied. On the glycan array, H10mall with Q226L showed dual binding specificity toward both α2,3- and α2,6 receptors (Figure 2F). H10sealG bound only α2,3 receptors, similar to the two avian A/H10 HA's (Figure 2G), but introduction of Q226L resulted in dual receptor specificity (Figure 2H). This is similar to H10mall with the Q226L substitution and H10sealNL that contained Q226L naturally. When both substitutions Q226L and G228S were introduced in H10sealG, dual receptor specificity was observed, and the avidity for shorter α2,6 targets was increased (Figure 2I). The binding preference of the H10sealG deletion mutant, which lacks an amino acid at position 228 but contains Q226L (H10sealG Q226L,Δ228), was similar to the Q226L mutant (Figure 2J).

Biolayer interferometry (BLI) was used to quantitatively analyze the binding of A/H10 seal influenza viruses, to human- and avian-type receptor analogs. BLI measurements on H10sealG showed that, like avian influenza viruses, it had significantly greater avidity for avian-type receptors than for human-type receptors (Figure 3A). The H10sealG Q226L mutant bound avian- and human-type receptors with similar avidity (Figure 3B). The H10sealG Q226L/G228S double mutant had a preference for binding human-type receptors (Figure 3C), and similar double substitutions were found in the HAs of 1957 and 1968 pandemic viruses by comparison with avian A/H2 and avian A/H3 viruses that were possibly their precursors (Connor et al., 1994; Liu et al., 2009). The H10sealG Q226L,Δ228 double mutant had very similar avidity for avian- and human-type receptors (Figure 3D).

BLI measurements on H10mall showed that although it had substantially greater avidity for avian-type receptors than for human-type receptors (Figure 3E), it bound human-type receptors more strongly than H10sealG. A previously isolated A/H10 avian influenza virus (A/mallard/Sweden/51/2002 A/H10N2) showed very similar binding properties to H10mall (Figure 3F). H10sealNL and the H10mall Q226L mutant both had approximately 10-fold higher avidity for human-type receptors than avian-type receptors (Figures 3G and 3H).

The binding properties of the control, human A/H3 A/Netherlands/213/2003 and the avian A/H5 A/Indonesia/5/2005 were also measured by BLI (Figures 3I and 3J). The 2003 seasonal A/H3 virus only bound human-type receptors, whereas the 2005 avian A/H5 virus only bound avian-type receptors.

Altogether, these results for the HAs of the H10 viruses demonstrated that the Q226L mutation was primarily responsible for the change in receptor-binding specificity of the seal influenza viruses from a preference for α2,3 receptors, to dual specificity for both α2,3- and α2,6 receptors or a preference for α2,6 receptors.

The Structures of the H10seal and H10mall Mutant HAs and the Complexes that They Form with Avian- and Human-Type Receptor Analogs

Purified seal A/H10N7 HA and its variants were crystallized in 3 different crystal forms under similar conditions and contained either a single or two biological trimers per crystallographic asymmetric unit (Table S2). Three out of the 4 potential glycosylation sites were visible in electron density maps.

The structure of the receptor-binding pocket of the H10sealG HA was similar to that of the human origin A/H10N8 HA (A/

Please cite this article in press as: Herfst et al., Hemagglutinin Traits Determine Transmission of Avian A/H10N7 Influenza Virus between Mammals, Cell Host & Microbe (2020), https://doi.org/10.1016/j.chom.2020.08.011

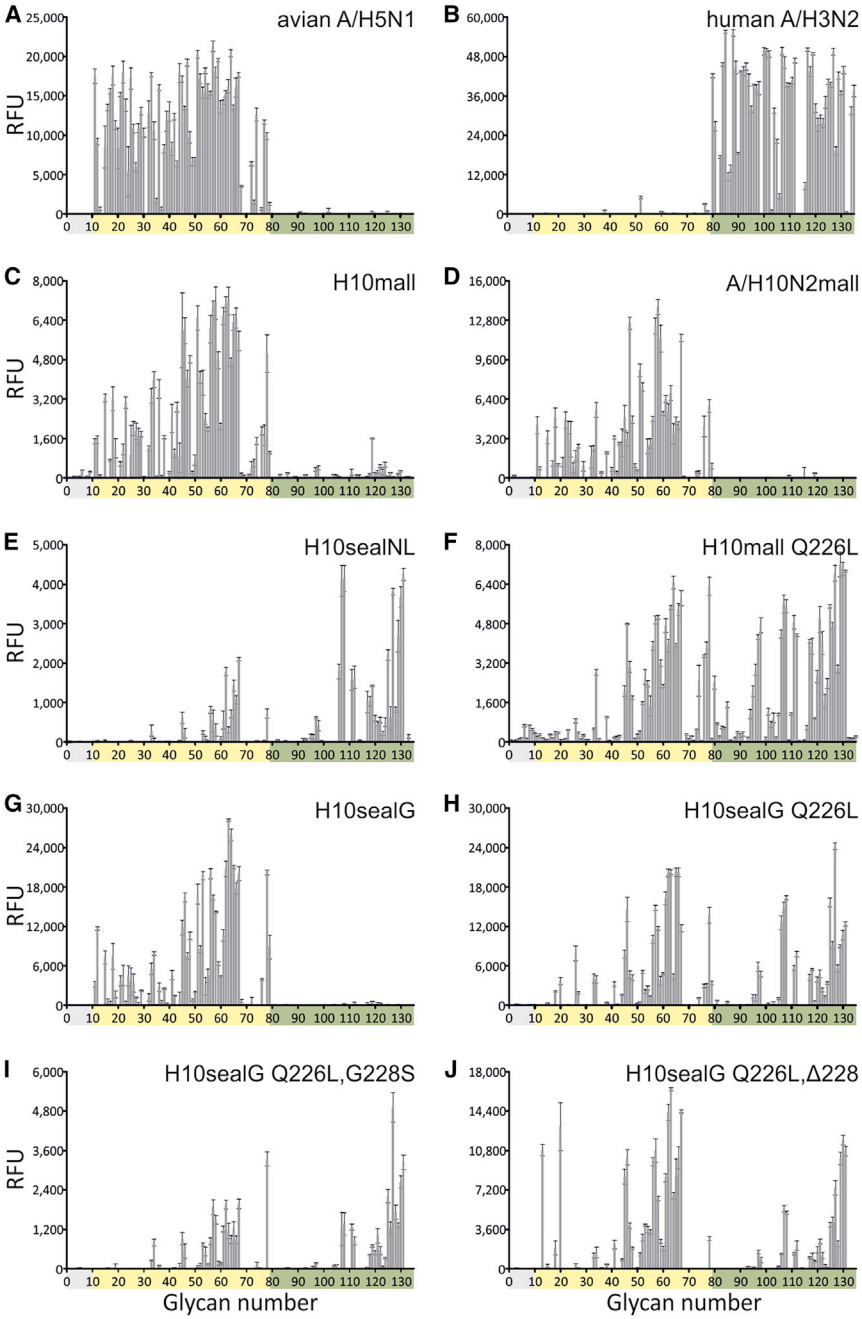

Figure 2. Receptor Specificities of Different Avian, Seal, and Mutant A/H10 Has

Glycan microarray analysis was used to determine the receptor specificities of A/Indonesia/05/2005 (A–J) (A/H5N1) (A), A/Netherlands/213/2003 (A/H3N2) (B), A/H10N7 HAmall (C), HA A/H10N2mall (D), H10sealNL (E), H10mall Q226L (F), H10sealG (G), H10sealG Q226L (H), H10sealG Q226L,G228S (I), and H10sealG Q226L,Δ228 (J). The mean signals and standard errors were calculated from 4 independent replicates. The data shown are representative of results from 2 independent assays. α2-3-linked sialosides (glycans 11 to 79 on the x axis) and α2-6-linked sialosides (glycans 80 to 135) are shown. Glycans 1 to 10 are non-sialylated controls. RFU, relative fluorescence units.

Jiangxi-Donghu/346/2013) and to that of H10sealNL (Vachieri et al., 2014) (Figures S3A and S3B). Similarly, the structures of the receptor-binding sites of the H10sealG Q226L mutant and of H10sealG Q226L/G228S double mutant were similar to that of the H10sealNL (Figures S3C and S3D). In contrast, the deletion of residue 228 changed the shape of the 220-loop resulting in a movement of about 2 Å in the position of the Leu-226 C-α (Figure S3E).

Avian-Type-Receptor-Binding Characteristics

The H10sealG has a glutamine at position 226 and binds the avian α2,3-linked sialic acid receptor in a *trans*-configuration (Figure 4A). This is the hallmark of avian HA binding to avian-type receptor and is associated with high affinity binding (Ha et al., 2001; Xiong et al., 2013a, 2013b). The observed binding mode features hydrophilic Gln-226 forming hydrogen bonds with both the Sia-1-Gal-2 glycosidic oxygen and the 4-hydroxyl group of Gal-2. This correlated with a 1-Å upward movement of the Gln-226 side chain from its position in the unbound HA structure (Figure 4A) as seen before (Xiong et al., 2013a) In addition, the distance between the 130-loop and the 220-loop decreased by about 0.5 Å in the HA-avian-type receptor complex compared with the unbound H10sealG structure. The bound avian-type receptor extends upward and exits the receptor-binding site toward the N terminus of the 190 helix.

In contrast, the HA of H10sealNL, which was transmissible via aerosols or respiratory droplets between ferrets, bound avian-type receptor in a *cis*-configuration similar to the configuration of avian-type receptors bound by the transmissible A/H5 mutant and human A/H7N9 HA (Xiong et al., 2013a, 2013b) (Figure 4B). Compared to the receptor analog bound in the *trans*-configuration, the Sia1-Gal2 glycosidic bond in the *cis*-configuration is rotated counterclockwise more than 90°. Consequently, instead of extending upward toward the N terminus of the 190 helix in the *trans*-configuration, the avian-type receptor exited from the side of the receptor-binding site in the *cis*-configuration over the 220 loop, almost parallel to the 190 helix (Figure 4B). In the *cis*-configuration the hydrophilic glycosidic bond is accommodated further from the hydrophobic leu-226 residue. The change in the conformation of the bound avian-type receptor from *trans* to *cis* often correlates with our observed decrease in affinity (Xiong et al., 2013a, 2013b)

The avian-type receptor also adopted a *cis*-configuration when bound to the H10sealG Q226L mutant and the H10sealG

Please cite this article in press as: Herfst et al., Hemagglutinin Traits Determine Transmission of Avian A/H10N7 Influenza Virus between Mammals, Cell Host & Microbe (2020), https://doi.org/10.1016/j.chom.2020.08.011

CellPress

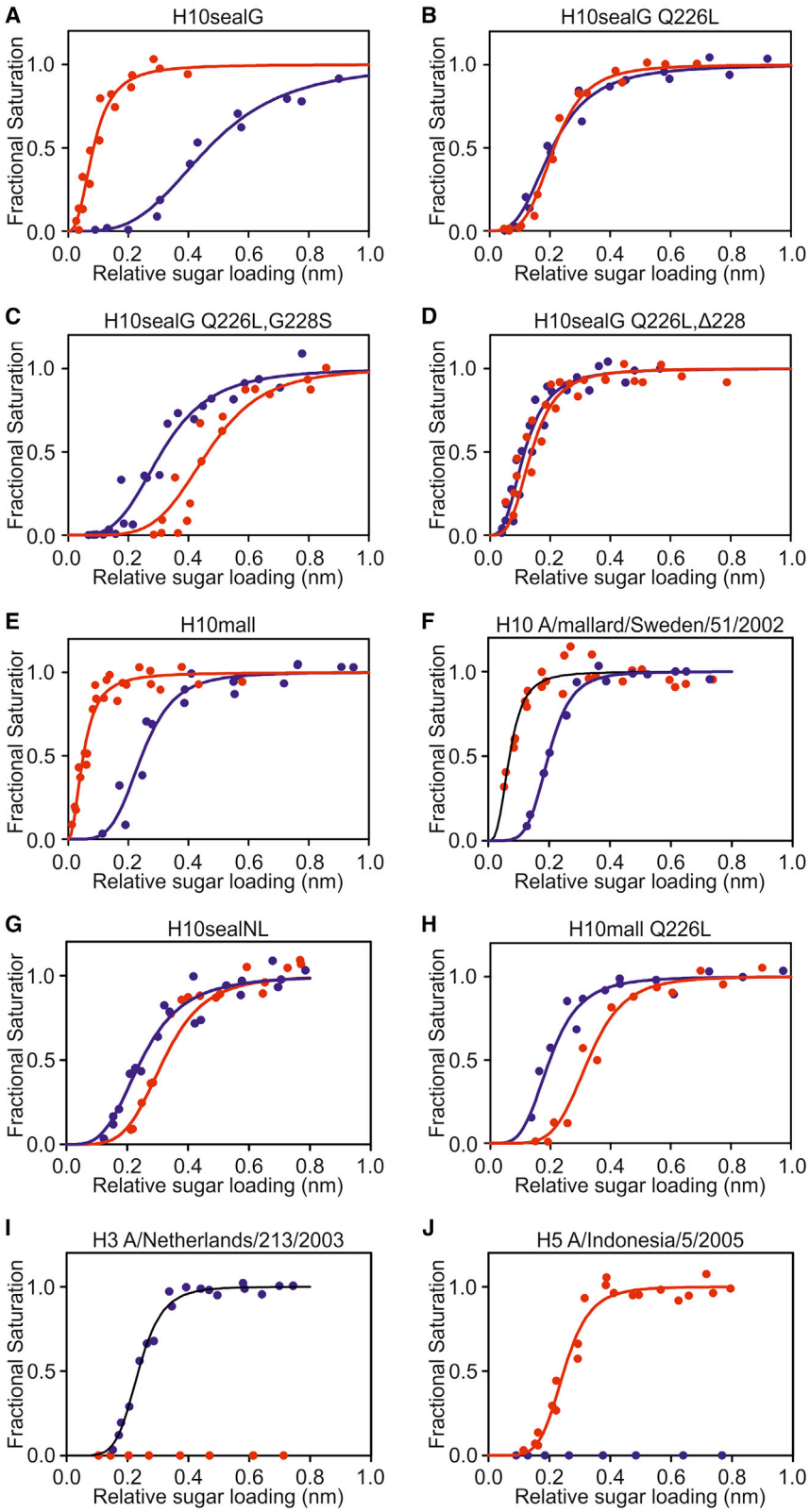

Figure 3. ■■■

Biolayer interferometry data of the binding of A/H10 seal and A/H10 mallard viruses and their variants to human- and avian-type receptor analogs (A–H) and control viruses A/Netherlands/213/2003 (A/H3N2) and A/Indonesia/05/2005 (A/H5N1) (I and J). The symbols shown in each diagram are the experimental data for the fractional saturations of the biosensors with various sugar loading levels by a fixed concentration of virus (1 nM). The solid curve is a fit of the experimental data to the Hill equation, which can be used to calculate an estimate of the binding avidity of a virus for a receptor. The binding of viruses to 30 kDa sialyglycopolymers containing α-2,3-sln (avian-type receptor analog) is in red. The binding of viruses to 30 kDa sialyglycopolymers containing α-2,6-sln (human-type receptor analog) is in blue. The H10sealG Q226L mutant binds avian and human receptors with similar avidity (B).This resulted from a 100-fold decrease in avidity for avian-type receptor and a 100-fold increase in avidity for human-type receptor. The Q226L/G228S double mutant preferred human-type receptor (C), which resulted from a 15,000-fold decrease in avidity for avian-type receptors coupled with a ~10-fold increase in avidity for human-type receptor. The Q226L,Δ228 double mutant has similar avidity for avian and human-type receptors resulting from a 10-fold decrease in avidity for avian-type receptor coupled with 3,000-fold increase in avidity for human-type receptors (D).

Q9

Please cite this article in press as: Herfst et al., Hemagglutinin Traits Determine Transmission of Avian A/H10N7 Influenza Virus between Mammals, Cell Host & Microbe (2020), https://doi.org/10.1016/j.chom.2020.08.011

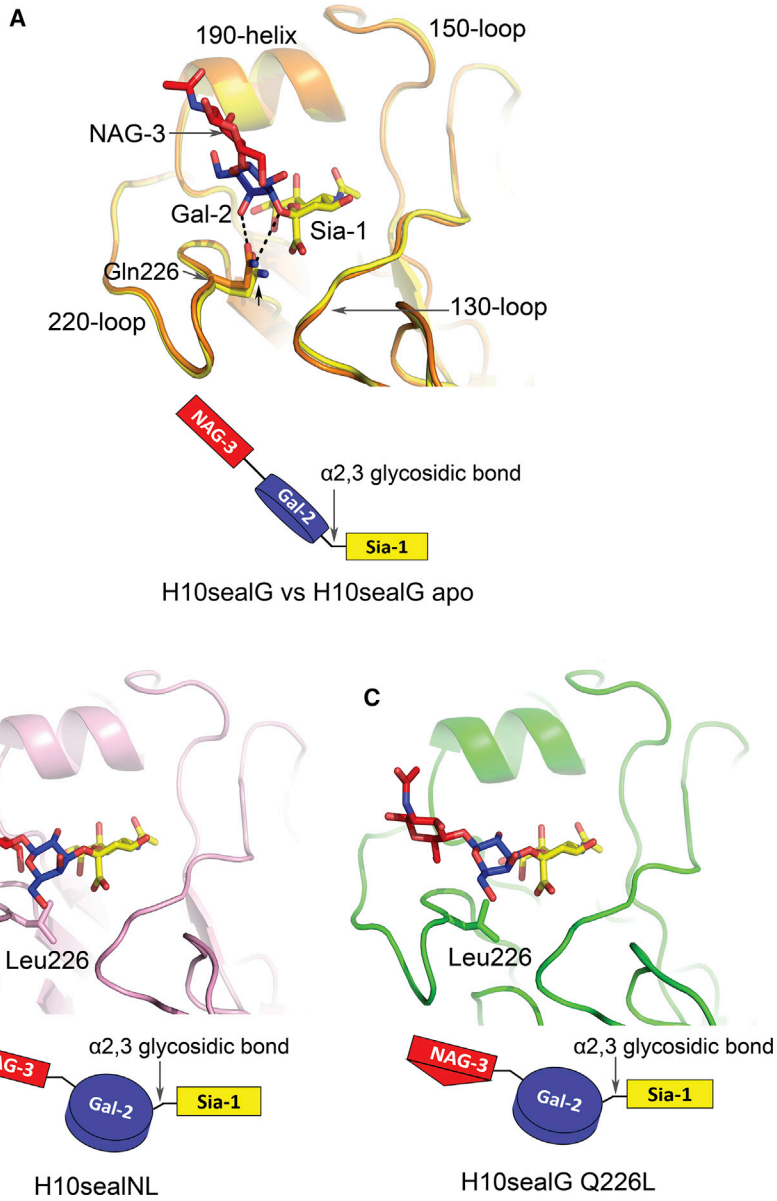

Figure 4. Avian-Type-Receptor-Binding Features of H10sealG, H10sealNL, and H10sealG Q226L

(A–C) The conformations of avian-type receptors bound to H10sealG, H10sealNL, and H10sealG Q226L and their schematic representations are shown in (A–C), respectively. The sialic acid, galactose, and N-acetylglucosamine of the receptor analogs are colored in yellow, blue, and red, respectively. The receptor-binding site of the avian-type receptor complex of H10sealG is superposed on the receptor-binding site of the apo structure of H10sealG (the distance between Cα of 224N and Cα of 136A decreased by about 0.5 A) (A). H10sealG is colored in orange in its complex structure and in yellow in its apo structure. HAsealNL is colored in pink (B). H10sealG Q226L mutant is colored in green (C).

Q226L/G228S double mutant as in the complexes formed by H10sealNL (Figures 4C and S4A). Alignments of the receptor-binding sites of the Q226L mutant and the Q226L/G228S mutant compared with that of the H10sealNL HA indicated that the orientation of Sia-1 and Gal-2 in the avian-type receptor complexes was similar.

The H10sealG Q226L,Δ228 mutant bound avian-type receptor in the *trans*-configuration (Figure S4B). Alignment of the Q226L and Q226L,Δ228 avian-type receptor complexes indicated that the bound sialic acid occupied a similar position relative to the 130-loop. The 220-loop of the deletion mutant was disordered between residues 217 and 226 (Figure S4B), and only density for sialic acid and galactose could be observed in the complex. The disordered 220 loop was accompanied by repositioning of Leu-226, which may facilitate binding of the receptor in the *trans*-configuration. A similar observation was made with an avian A/H7 HA with a deleted 220-loop in which the avian-type receptor also adopted a *trans*-configuration (Yang et al., 2010).

Human-Type-Receptor-Binding Characteristics

In line with previous observations made with an A/H5 aerosol or respiratory droplet-transmissible mutant, the Q226L substitution in the receptor-binding site of A/H10 seal HAs correlated with the loss of a hydrogen bond between the side chain of 226Gln and the carboxylate group of Sia-1 (Xiong et al., 2013a). 226Leu interacted with C6 and C4 of the hydrophobic face of the Gal-2 sugar ring, and there is a rotation of ~90° about the Sia1-Gal2 glycosidic bond. The Gal-2 and NAG-3 saccharides also rotated~90° toward the 190 helix, and as a result, the plane of the di-saccharide was perpendicular to the plane of the Sia-1 sugar ring. A folded-back conformation of the human-type receptor was observed in the H10sealG Q226L mutant, the aerosol or respiratory droplet-transmissible H10sealNL, and the H10sealG Q226L/G228S mutant (Figures 5A, 5B, and S5A). This was consistent with tighter human-type receptor binding and with transmission via aerosol or respiratory droplets, properties shared with pandemic A/H1, A/H2, and A/H3 and aerosol or respiratory droplet-transmissible A/H5 HAs (Eisen et al., 1997; Gamblin et al., 2004; Liu et al., 2009; Xiong et al., 2013a).

Previous work has shown that the human-type receptor is bound by the human A/H7N9 HA in a less vertical orientation than the human-type receptors bound to pandemic A/H1, A/H2, A/H3 Has, and aerosol or respiratory droplet-transmissible A/H5 HA. It has been proposed that this orientation of human-type receptor bound to A/H7 HA may be due to the 150-loop that protrudes into the receptor-binding site of HAs of the A/H7, A/H10, and A/H15 clade (Xiong et al., 2013b). However, in

Please cite this article in press as: Herfst et al., Hemagglutinin Traits Determine Transmission of Avian A/H10N7 Influenza Virus between Mammals, Cell Host & Microbe (2020), https://doi.org/10.1016/j.chom.2020.08.011

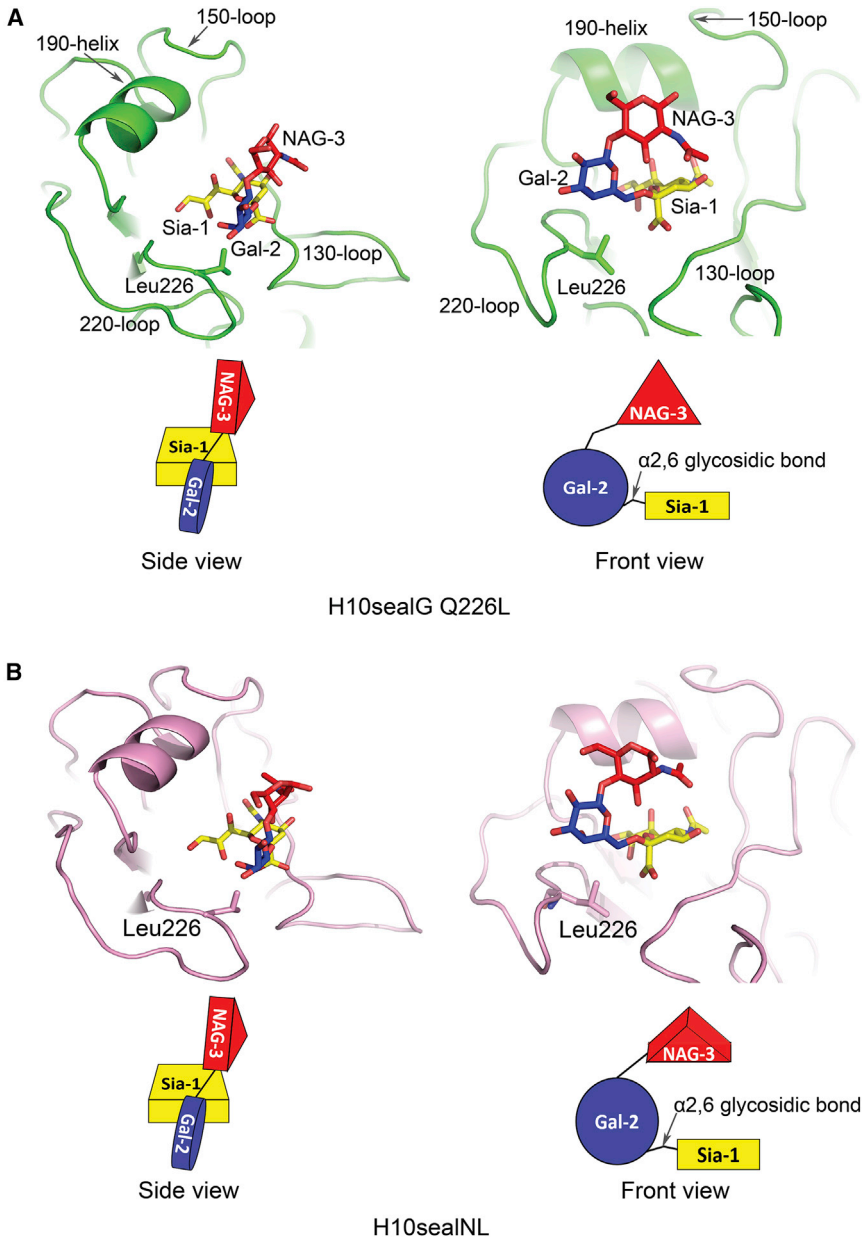

Figure 5. Human-Type Receptor-Binding Features of H10sealG Q226L and H10sealNL

The side and front views of conformations of human-type receptors bound to H10sealG Q226L and H10sealNL are shown on the left and right sides of (A and B), respectively. The schematic representations of the conformations of the human-type receptors are shown in (A and B) as well. The sialic acid, galactose, and N-acetylglucosamine of receptor analog are colored in yellow, blue, and red individually. H10sealG Q226L is colored in green in its complex structure (A). HAsealNL is colored in pink (B).

seal A/H10 HA, which also has an extended 150-loop, the human-type receptor adopted a conformation similar to that seen for this receptor in pandemic A/H1, A/H2, A/H3, and aerosol or respiratory droplet-transmissible A/H5 HAs (Figures S6A–S6E).

The H10sealG Q226L mutant and the H10sealG Q226L/G228S double mutant bind human-type receptor in a similar way to H10sealNL HA (Figures S6F and S6G). Noticeably, the positions of Sia-1 in the different HA monomers of H10sealG Q226L/G228S mutant (carboxylate group rmsd 1.4–2.4Å) are slightly different in comparison with the sialic acids bound in the H10sealG Q226L mutant (carboxylate group rmsd 0.7Å). This heterogeneity is reflected in weaker binding of the human-type receptor observed in BLI.

The H10sealG binds human-type receptor in *cis*-configuration (Figure S4C), similar to wild-type avian A/H5 and A/H7 HA's, with the receptor exiting from the front of the site (Xiong et al., 2013a, 2013b). There was a 5° to 10° upward rotation of the glycosidic bond of sialic acid to galactose in H10sealG compared with human-type receptors bound to avian A/H5 and avian A/H7 HAs.

Binding of human-type receptor by the H10sealG Q226L,Δ228 double mutant involved a disordered 220-loop (Figure S5B), (rmsd 6.5 Å) and of the conformation of the 220-loop in the H10sealG Q226L Δ228, double mutant and alteration of the position of Leu-226 provided space for the bound human-type receptor to adopt different configurations. By comparison with human-type receptor bound to the H10sealG HA, Gal2-NAG3 residues of the bound human-type receptor in the H10sealG Q226L, Δ228 mutant complex were rotated ~180° around the glycosidic bond (Figure S5B). In this arrangement the ε amino group of Lys137 potentially makes hydrogen bonds with the 5′O and 4'OH of Gal-2 that could stabilize this conformation.

Structural Flexibility and Calcium Binding of H10 Seal HA's

Despite showing overall similarity to the previously characterized mallard (A/H10N7) and human (A/H10N8) HA structures (Vachieri et al., 2014), the receptor-binding domains of the seal A/H10 HAs varied in positions and orientations relative to the fusion domains (rmsd up to 4.2 Å). By comparison, these relative orientations and positions in human A/H10 HA were less variable (rmsd ~ 0.9 Å). Structural alignment indicated that the relative positions and orientations of the α-helical structure between residues $HA_1$104 and $HA_1$114, the 110-helix, also varied in different subunits of the H10sealG Gln226Leu mutant. Examination of this region revealed a calcium-binding site in which the calcium ion was coordinated by the side chains of Glu114 in the 110-helix and of Glu64 of HA_2 in the same subunit (Figure 6). In addition, the side chain of HA_2 Asn79 of a neighboring subunit and the acetyl carbonyl of the first N-acetyl glucosamine in the carbohydrate

Please cite this article in press as: Herfst et al., Hemagglutinin Traits Determine Transmission of Avian A/H10N7 Influenza Virus between Mammals, Cell Host & Microbe (2020), https://doi.org/10.1016/j.chom.2020.08.011

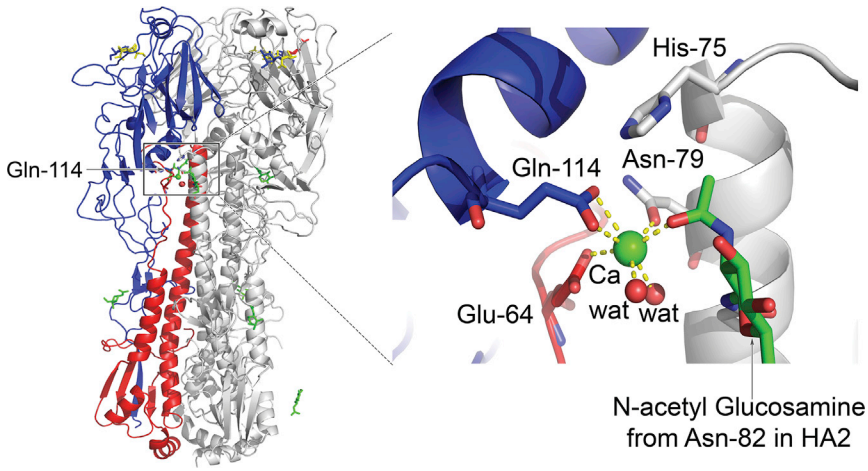

Figure 6. Calcium Binding to A/H10 Seal HA
The calcium-binding site of A/H10 seal HA is shown on the right side. The green sphere represents the calcium ion and the red sphere represents the water molecule. The side chains of the residues, which coordinate with the calcium are shown and the interactions between them and calcium are represented as yellow dash lines. Sugars are colored in green. A ribbon representation of the crystal structure of H10sealG Q226L's complex with avian-type receptor analog is shown on the left side. HA_1 and HA_2 from one monomer are colored in blue and red, respectively and another two monomers in the HA trimer are colored in gray. The glycosylation in this structure is colored in green. The sialic acid, galactose, and N-acetylglucosamine of the receptor analog are colored in yellow, blue, and red individually.

side chain attached to HA_2 Asn82 of the same neighboring subunit, also coordinated the calcium. The calcium coordination had pentagonal bipyramidal geometry that closely resembled the calcium-binding site in an EF hand (Kretsinger and Barry, 1975) (Figure 6). Sequence and structural comparisons of the phylogenetically related A/H7 and A/H15 HAs indicated that the orientation of the side chain of Glu114 in the putative calcium-binding sites changed as a result of the absence of His75 from HA_2 of these 2 subtypes (Tzarum et al., 2017b; Xiong et al., 2013b). As a result, calcium was not bound by these HAs.

The observation that calcium coordinates residues of the receptor-binding domain and residues of HA_2 of the same and neighboring HA subunits, suggested that bound calcium may influence HA stability. Thermal denaturation experiments gave results consistent with this suggestion by demonstrating that the presence of 2 mM calcium significantly increased the thermal stability of H10sealG 226Q/228G (Tm from 61°C to 69°C), the H10sealG Q226L mutant (Tm from 61°C to 69°C), the H10sealG Q226L,Δ228 mutant (Tm from 62°C to 67°C), and the H10sealG Q226L/G228S double mutant (Tm from 63°C to 69°C) (Figure S7). In contrast, 2mM calcium did not affect the stability of HA from A/Aichi/2/68 H3N2 X-31 strain (Figure S7). The results of tryptophan fluorescence assays of denaturation by urea were also consistent with calcium enhancing the stability of A/H10 HA's at room temperature (Figure S8). Calcium stabilized A/H10 human HA and H10sealG Q226L mutant but had little effect on the stability of A/H7 HA and no effect on the stability of X-31 A/H3N2 HA or A/H5 HA or on the stability of transmissible H10sealNL HA, (Figure S8). The fluorometric titration data indicate that H10sealG and A/H10 human HA bind calcium with micromolar affinities (Figure S9).

The crystal structures of all these HAs suggest a rationale for the results of the stability assays. Electron density for the coordinated calcium ion was observed in crystal structures of A/H10 human, H10mall, and most A/H10 seal HAs. In contrast, the aerosol- or respiratory-droplet-transmissible H10sealNL and A/H7 HAs in the same clade show no electron density for calcium in their putative binding sites.

The different calcium-binding characteristics observed between H10sealNL and H10sealG could result from two sequence differences in H10sealNL, namely, serine 212 instead of asparagine and isoleucine 244 instead of threonine in the interface between the receptor-binding subdomains. These substitutions influence the relative orientations of the receptor binding, esterase and fusion subdomains, and the position and orientation of Glu114. As a consequence, the loss of interaction between Glu114 and His75 appears to prevent Ca^{2+} binding by H10sealNL.

Despite the effect of calcium binding on HA stability, the results of proteolysis assays indicate that calcium has no detectable effect on the pH of the conformational change of H10sealG Gln226Leu HA (Figure S10) nor does it influence the thermal stability of H10sealG Gln226Leu HA at pH 6.0 (Figure S10).

Membrane Fusion by A/H10N7 Viruses

Attachment of influenza viruses to sialic acid receptors on the cell surface is followed by internalization into endosomes, where, in the low-pH activated conformation, HA mediates fusion of the viral and endosomal membranes, resulting in the release of the virus genome into the cytoplasm (Skehel and Wiley, 2000). Previous work has shown that the HAs of aerosol or respiratory droplet-transmissible influenza viruses are comparatively stable, e.g., in studies on mammalian adaptation of avian A/H5N1 viruses. (Herfst et al., 2012; Imai et al., 2012). In another study on the emergence of the swine-origin pH1N1 influenza virus in humans in 2009, it was shown that the HA stability increased during the evolution of A/H1N1 from precursors in swine, to the early pH1N1 human cases and to the later human isolates (Russier et al., 2016).

The fusion pH of H10sealNL and H10mall was estimated in syncytia formation assays. Fusion by H10mall was activated at pH $\leq$5.5 (Figure 7). In contrast, the H10sealNL HA required a pH for fusion of <5.2. To determine the substitutions responsible for changes in pH of fusion, all amino acids that were different between H10mall and H10sealNL (18 in total) were introduced individually in H10mall (Table S3). The Q226L substitution in H10mall destabilized HA to pH <5.7. Two-amino-acid substitutions that had the most stabilizing effect on H10mall; T244I and E74D (HA_2) (Table S3) were introduced in H10mall Q226L. This resulted in a decreased pH of fusion of 5.2, suggesting that

Please cite this article in press as: Herfst et al., Hemagglutinin Traits Determine Transmission of Avian A/H10N7 Influenza Virus between Mammals, Cell Host & Microbe (2020), https://doi.org/10.1016/j.chom.2020.08.011

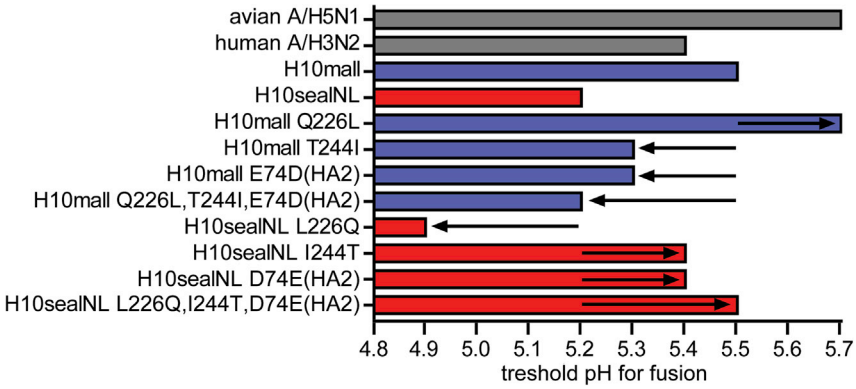

Figure 7. Analysis of the pH Threshold for Fusion of Wild-Type and Mutant A/H10 HA Proteins

Syncytium formation in Vero-118 cells upon expression of wild-type or mutant HA proteins after exposure to different pH. Visual inspection of the cell cultures for the presence of syncytia was used to determine the pH of fusion. The bars indicate the thresholds of pH at which fusion was detected microscopically. The arrows indicate the stability change compared with the parental (WT) H10mall or H10seal. An avian A/H5N1 (A/Indonesia/5/2005) and human A/H3N2 (A/Netherlands/213/2003) HA were included as controls.

three-amino-acid substitutions were sufficient to change the receptor-binding specificity and acid stability of H10mall toward that of H10sealNL (Figure 7). As expected, reverse substitutions in H10sealNL had the opposite effect: L226Q stabilized the HA (pH 4.9), whereas I244T and D74E (HA_2) reverted the stability of the HA (pH 5.4 for both). The triple mutant L226Q, I244T, and D74E (HA_2) in H10sealNL had the same threshold pH of fusion as HAmall, i.e., pH 5.5 (Figure 7).

DISCUSSION

The outbreak of A/H10N7 influenza in seals in 2014 provided an opportunity to study the natural evolution of an avian influenza virus in a mammalian host. This is of interest since it reveals processes involved in the direct transmission of an avian influenza virus to mammals and then between thousands of individuals within a population, and because infected seals could potentially be novel intermediates in the transmission of avian influenza viruses to other mammals including humans. The exact transmission route between seals is unknown, but it is likely to occur via aerosols or respiratory droplets, most probably while the seals are resting on land. However, direct contact transmission between seals can also not be excluded because seals are highly social, and they interact with each other regularly.

Our results indicate that the receptor-binding properties of the HA glycoprotein of the avian influenza virus changed in the establishment of the infection in seals. The avidities and specificities of the changed HA were detailed by microarray analyses using a large number of sialoside receptor analogs, by quantitative, biolayer interferometry assays of receptor analog binding by virus, and by X-ray crystallography of complexes formed between HA and receptor analogs. Together they showed that the changes required for infection of seals caused a decrease in the avidity of the virus for avian-type receptors and an increase in its preference for human-type receptors. The changes were caused by substitutions in the 220-loop that forms one edge of the receptor-binding pocket, in particular the amino-acid substitution Q226L. This change also occurred in the HA of an aerosol or respiratory droplet-transmissible mutant of the initial avian influenza virus that infected seals; it was found when the initial virus replicated in ferrets, and it occurred in viruses isolated in the late phases of the outbreak presumably as a result of selection during the outbreak. This observation is similar to the human A/H2N2 viruses isolated in the first year of the 1957 pandemic. The first viruses to infect humans contained an avian receptor-binding preference, however, likely as the result of adaptation to replication and transmission in humans, the viruses mutated rapidly, thereby gaining human receptor-binding preference (Pappas et al., 2010). This suggests that the efficient introduction of a new avian influenza virus in mammals does not necessarily require a human receptor-binding phenotype, but this trait may emerge later during the outbreak as the result of mutation and selection.

A/H10N8 viruses were found to cause serious infections of a small number of humans in China in 2013 (Chen et al., 2014). One of the studies of the HA of this virus indicated that by comparison with an avian influenza virus HA that strongly preferred avian-type receptor, the HA of the virus isolated from humans, bound avian and human-type receptors with similar affinity (Vachieri et al., 2014). Another study, however, concluded that the A/H10N8 virus isolated from infected humans retained the receptor-binding properties of an avian influenza virus (Zhang et al., 2015). The reasons for these different conclusions remain to be determined but they may be related in part to differences in the binding assays and the HA protein used (baculovirus-expressed HA or HAs in virus particles). The study of Zhang et al. also involved site specific substitutions to introduce the amino-acid substitutions Q226L and G228S. The conclusion from microarray receptor-binding assays was that these substitutions were insufficient to change the preference of the A/H10N8 virus for avian-type receptor (Zhang et al., 2015). The human and seal influenza viruses appear, therefore, to differ in this regard also. As well as substitutions in the 220-loop, additional substitutions were made in the 150-loop in a second study, and triple mutants were found to prefer human-type receptors (Tzarum et al., 2017a).

HA in the A/H7, A/H10, A/H15 clade, uniquely among HA's of the five clades into which influenza A viruses are divided on the basis of genetic, antigenic and structural characteristics, contain insertions of amino acids in the 150-loop (Nobusawa et al., 1991), a structural element in the opposite edge of the receptor-binding site from the 220-loop. As a consequence, the extended loops protrude into the receptor-binding site and possibly interfere with binding of human-type receptor in the folded-back conformation (Russell et al., 2004). From the results with the constructed mutants, it was concluded that substitution

of residues with shorter amino-acid side chains in the 150-loop resulted in human-type receptor binding (Tzarum et al., 2017a). Again, these would be different requirements from those observed for the A/H10N7 viruses from seals.

From our observations on the seal influenza viruses, substitutions in the 150-loop are not selected in aerosol or respiratory droplet transmitted mutants, nor, importantly, during the development of the extensive seal outbreak. On the contrary, the mutation Q226L was selected in both cases and this is consistent with the importance of this mutation in the evolution of the HA of the viruses that caused the A/H2 pandemic of 1957 and the A/H3 pandemic of 1968 (Connor et al., 1994).

Substitutions in HA related to the pH of fusion or thermostability have previously been shown to increase aerosol or respiratory droplet transmission of HPAI A/H5N1 and also the 2009 pandemic A/H1N1 (Imai et al., 2012; Linster et al., 2014; Russier et al., 2017). A set of three substitutions, including Q226L, between H10sealNL and H10mall, was also found to affect A/H10 HA stability. Introduction of leucine at residue 226 as a result of mammalian adaptation during circulation in seals resulted in a less stable HA, as previously observed for A/H5N1 and A/H7N9 (Linster et al., 2014; Schrauwen et al., 2016). This destabilizing effect was compensated by T244I and E74D (HA_2) substitutions, which emerged during circulation in the seal population. It is also possible that the HA stability phenotype as measured in fusion and temperature stability assays may co-vary with other, as yet unknown phenotypes, such as stability of HA in aerosols, resistance to drought, stability in mucus, or resistance to changes in pH in the host environment. It should also be noted that H10mall, despite its relatively unstable HA and dual receptor-binding preference for both α2,3 and α2,6 sialic acid, was capable of transmitting through the air, although very inefficient (in one out of eight donor-recipient pairs). Similar findings were obtained recently for a gull-origin A/H10N7 virus that also had a limited aerosol or respiratory droplet-transmissibility in the ferret model (Guan et al., 2019).

The viral phenotypes that changed as a result of the seal adaptation of the avian A/H10N7 virus resemble those that had to change for the aerosol or respiratory droplet-transmissible A/H5N1 virus, although for A/H10N7, there was no indication that adaptation of the polymerase complex was required. Despite many amino-acid differences between the avian and seal virus polymerase complexes, no differences were observed in the replication kinetics of the avian and seal viruses in seal cells (Table S1 and Figure S2). For adaptation of avian influenza viruses to humans, viral host factors such as importins and ANP32 have been discovered previously, but the possible role of such or other host factors for seals is yet unknown (Gabriel et al., 2008; Long et al., 2016).

H10 subtype influenza viruses have shown the potential not only to infect several mammalian species, including humans, but also to spread efficiently between and among mammals, allowing adaptation to new mammalian hosts. In this study, the adaptation to seals of an avian-origin A/H10N7 virus was studied throughout a series of outbreaks, infecting thousands of individuals, revealing that the same changes in viral properties were required as previously described for HPAI A/H5N1 (Imai et al., 2012; Linster et al., 2014). In addition, changes in HA stability have now been demonstrated for a second avian influenza virus subtype to be of importance to gain aerosol or respiratory droplet-transmissibility between mammals. Our observations help us to increase our basic understanding of influenza virus transmission and also suggest that the emergence of animal influenza viruses with increased HA stability, in addition to human-type receptor preference and high polymerase activity, should be monitored in surveillance programs aimed to identify zoonotic threats.

STAR★METHODS

Detailed methods are provided in the online version of this paper and include the following:

- KEY RESOURCES TABLE
- RESOURCE AVAILABILITY
  - Lead Contact
  - Materials availability
  - Data and code availability
- EXPERIMENTAL MODEL AND SUBJECT DETAILS
  - Experimental Animals
- METHOD DETAILS
  - Biocontainment
  - Viruses
  - Virus Titration in MDCK Cells
  - Transmission of A/H10N7 Virus via Aerosols or Respiratory Droplets in the Ferret Model
  - Serology
  - Purification of HAs
  - Crystallization
  - Virus Preparation for Biolayer Interferometry
  - Biolayer Interferometry
  - Virus Preparation for Glycan Array
  - Glycan Array Fabrication
  - Virus Labeling and Binding Assays
  - CD Measurements
  - Trp Fluorescence Assay
  - Calcium Binding Assays
  - pH Dependent Proteolysis Experiment
  - Minigenome Assay
  - Plaque Assay
  - Replication Kinetics in Seal Cells
  - Enzyme-Linked Lectin Assay
  - Fusion (Acid Stability) Assay
- QUANTIFICATION AND STATISTICAL ANALYSIS

SUPPLEMENTAL INFORMATION

Supplemental Information can be found online at https://doi.org/10.1016/j.chom.2020.08.011.

ACKNOWLEDGMENTS

We are grateful to M. Peiris, University of Hong Kong, who provided A/Indonesia/5/2005 with permission from I. Kandun of the Indonesian Government. This work was supported by NIH/NIAID contract HHSN272201400008C to R.A.M.F., Nwo Vidi Grant (contract number 91715372) to S.H., Volkswagen Foundation to E.v.d.V., NIH grant R01 AI114730 to J.C.P., and the Francis Crick Institute, which receives its core funding from the Wellcome Trust (FC001078 and FC001143). We acknowledge Phil Walker and Andrew Purkiss

of the Structural Biology Science Technology Platform for X-ray data collection and other crystallographic and computational support.

AUTHOR CONTRIBUTIONS

S.H., J.Z., J.C.P., J.J.S., and R.A.M.F. conceived, designed, and supervised the project. S.H., J.Z., M.R., R.M., P.L., T.M.B., M.I.J.S., D.d.M., J.M.v.d.B., and M.E.R. designed and conducted experiments. S.R.M., S.J.G., X.X., W.P., R.B., E.v.d.V., and A.D.M.E.O. helped with analysis, interpretation of data, and manuscript reviewing and editing. S.H., J.Z., J.C.P., J.J.S., and R.A.M.F. wrote the original draft of the manuscript. All authors read and approved the final manuscript.

DECLARATION OF INTERESTS

A.D.M.E.O. is Chief Scientific Officer at Viroclinics Biosciences and is ad hoc Scientific Advisory Board member of pharmaceutical companies for influenza virus vaccines and antivirals.

Received: November 28, 2019
Revised: June 4, 2020
Accepted: August 26, 2020
Published: October 7, 2020

REFERENCES

Adams, P.D., Afonine, P.V., Bunkóczi, G., Chen, V.B., Davis, I.W., Echols, N., Headd, J.J., Hung, L.W., Kapral, G.J., Grosse-Kunstleve, R.W., et al. (2010). PHENIX: a comprehensive Python-based system for macromolecular structure solution. Acta Crystallogr. D Biol. Crystallogr. *66*, 213–221.

Arzey, G.G., Kirkland, P.D., Arzey, K.E., Frost, M., Maywood, P., Conaty, S., Hurt, A.C., Deng, Y.M., Iannello, P., Barr, I., et al. (2012). Influenza virus A (H10N7) in chickens and poultry abattoir workers, Australia. Emerg. Infect. Dis. *18*, 814–816.

Bodewes, R., Bestebroer, T.M., van der Vries, E., Verhagen, J.H., Herfst, S., Koopmans, M.P., Fouchier, R.A., Pfankuche, V.M., Wohlsein, P., Siebert, U., et al. (2015). Avian Influenza A(H10N7) virus-associated mass deaths among harbor seals. Emerg. Infect. Dis. *21*, 720–722.

Bodewes, R., Zohari, S., Krog, J.S., Hall, M.D., Harder, T.C., Bestebroer, T.M., van de Bildt, M.W.G., Spronken, M.I., Larsen, L.E., Siebert, U., et al. (2016). Spatiotemporal analysis of the genetic diversity of seal influenza A(H10N7) virus, Northwestern Europe. J. Virol. *90*, 4269–4277.

Chen, H., Yuan, H., Gao, R., Zhang, J., Wang, D., Xiong, Y., Fan, G., Yang, F., Li, X., Zhou, J., et al. (2014). Clinical and epidemiological characteristics of a fatal case of avian influenza A H10N8 virus infection: a descriptive study. Lancet *383*, 714–721.

Chutinimitkul, S., van Riel, D., Munster, V.J., van den Brand, J.M., Rimmelzwaan, G.F., Kuiken, T., Osterhaus, A.D., Fouchier, R.A., and de Wit, E. (2010). In vitro assessment of attachment pattern and replication efficiency of H5N1 influenza A viruses with altered receptor specificity. J. Virol. *84*, 6825–6833.

Collaborative Computational Project, Number 4 (1994). The CCP4 suite: programs for protein crystallography. Acta Crystallogr. D Biol. Crystallogr. *50*, 760–763.

Connor, R.J., Kawaoka, Y., Webster, R.G., and Paulson, J.C. (1994). Receptor specificity in human, avian, and equine H2 and H3 influenza virus isolates. Q14 Virology *205*, 17–23.

de Wit, E., Munster, V.J., van Riel, D., Beyer, W.E., Rimmelzwaan, G.F., Kuiken, T., Osterhaus, A.D., and Fouchier, R.A. (2010). Molecular determinants of adaptation of highly pathogenic avian influenza H7N7 viruses to efficient replication in the human host. J. Virol. *84*, 1597–1606.

de Wit, E., Spronken, M.I., Bestebroer, T.M., Rimmelzwaan, G.F., Osterhaus, A.D., and Fouchier, R.A. (2004). Efficient generation and growth of influenza virus A/PR/8/34 from eight cDNA fragments. Virus Res. *103*, 155–161.

Dunn, J.J., Krippl, B., Bernstein, K.E., Westphal, H., and Studier, F.W. (1988). Targeting bacteriophage T7 RNA polymerase to the mammalian cell nucleus. Gene *68*, 259–266.

Eisen, M.B., Sabesan, S., Skehel, J.J., and Wiley, D.C. (1997). Binding of the influenza A virus to cell-surface receptors: structures of five hemagglutinin-sialyloligosaccharide complexes determined by x-ray crystallography. Virology *232*, 19–31.

Emsley, P., and Cowtan, K. (2004). Coot: model-building tools for molecular graphics. Acta Crystallogr. D Biol. Crystallogr. *60*, 2126–2132.

Gabriel, G., Herwig, A., and Klenk, H.D. (2008). Interaction of polymerase subunit PB2 and NP with importin alpha1 is a determinant of host range of influenza A virus. PLoS Pathog. *4*, e11.

Gamblin, S.J., Haire, L.F., Russell, R.J., Stevens, D.J., Xiao, B., Ha, Y., Vasisht, N., Steinhauer, D.A., Daniels, R.S., Elliot, A., et al. (2004). The structure and receptor binding properties of the 1918 influenza hemagglutinin. Science *303*, 1838–1842.

Gao, G.F. (2018). From "A"IV to "Z"IKV: attacks from emerging and re-emerging pathogens. Cell *172*, 1157–1159.

Guan, M., Hall, J.S., Zhang, X., Dusek, R.J., Olivier, A.K., Liu, L., Li, L., Krauss, S., Danner, A., Li, T., et al. (2019). Aerosol transmission of gull-origin Iceland Subtype H10N7 influenza A virus in ferrets. J. Virol. *93*, e00282–19.

Ha, Y., Stevens, D.J., Skehel, J.J., and Wiley, D.C. (2001). X-ray structures of H5 avian and H9 swine influenza virus hemagglutinins bound to avian and human receptor analogs. Proc. Natl. Acad. Sci. USA *98*, 11181–11186.

Herfst, S., Mas, V., Ver, L.S., Wierda, R.J., Osterhaus, A.D., Fouchier, R.A., and Melero, J.A. (2008). Low-pH-induced membrane fusion mediated by human Metapneumovirus F protein is a rare, strain-dependent phenomenon. J. Virol. *82*, 8891–8895.

Herfst, S., Schrauwen, E.J., Linster, M., Chutinimitkul, S., de Wit, E., Munster, V.J., Sorrell, E.M., Bestebroer, T.M., Burke, D.F., Smith, D.J., et al. (2012). Airborne transmission of influenza A/H5N1 virus between ferrets. Science *336*, 1534–1541.

Imai, M., Watanabe, T., Hatta, M., Das, S.C., Ozawa, M., Shinya, K., Zhong, G., Hanson, A., Katsura, H., Watanabe, S., et al. (2012). Experimental adaptation of an influenza H5 HA confers respiratory droplet transmission to a reassortant H5 HA/H1N1 virus in ferrets. Nature *486*, 420–428.

Klingeborn, B., Englund, L., Rott, R., Juntti, N., and Rockborn, G. (1985). An avian influenza A virus killing a mammalian species–the mink. Brief report. Arch. Virol. *86*, 347–351.

Kretsinger, R.H., and Barry, C.D. (1975). The predicted structure of the calcium-binding component of troponin. Biochim. Biophys. Acta *405*, 40–52.

Krog, J.S., Hansen, M.S., Holm, E., Hjulsager, C.K., Chriél, M., Pedersen, K., Andresen, L.O., Abildstrøm, M., Jensen, T.H., and Larsen, L.E. (2015). Influenza A(H10N7) virus in dead harbor seals, Denmark. Emerg. Infect. Dis. *21*, 684–687.

Lin, Y.P., Xiong, X., Wharton, S.A., Martin, S.R., Coombs, P.J., Vachieri, S.G., Christodoulou, E., Walker, P.A., Liu, J., Skehel, J.J., et al. (2012). Evolution of the receptor binding properties of the influenza A(H3N2) hemagglutinin. Proc. Natl. Acad. Sci. USA *109*, 21474–21479. Q15

Linster, M., van Boheemen, S., de Graaf, M., Schrauwen, E.J.A., Lexmond, P., Mänz, B., Bestebroer, T.M., Baumann, J., van Riel, D., Rimmelzwaan, G.F., et al. (2014). Identification, characterization, and natural selection of mutations driving airborne transmission of A/H5N1 virus. Cell *157*, 329–339.

Liu, J., Stevens, D.J., Haire, L.F., Walker, P.A., Coombs, P.J., Russell, R.J., Gamblin, S.J., and Skehel, J.J. (2009). Structures of receptor complexes formed by hemagglutinins from the Asian Influenza pandemic of 1957. Proc. Natl. Acad. Sci. USA *106*, 17175–17180.

Long, J.S., Giotis, E.S., Moncorgé, O., Frise, R., Mistry, B., James, J., Morisson, M., Iqbal, M., Vignal, A., Skinner, M.A., and Barclay, W.S. (2016). Species difference in ANP32A underlies influenza A virus polymerase host restriction. Nature *529*, 101–104.

Ma, W., García-Sastre, A., and Schwemmle, M. (2015). Expected and unexpected features of the newly discovered bat influenza A-like viruses. PLoS Pathog. *11*, e1004819.

Matrosovich, M., Matrosovich, T., Garten, W., and Klenk, H.D. (2006). New low-viscosity overlay medium for viral plaque assays. Virol. J. *3*, 63.

Munster, V.J., de Wit, E., van den Brand, J.M., Herfst, S., Schrauwen, E.J., Bestebroer, T.M., van de Vijver, D., Boucher, C.A., Koopmans, M., Rimmelzwaan, G.F., et al. (2009). Pathogenesis and transmission of swine-origin 2009 A(H1N1) influenza virus in ferrets. Science *325*, 481–483.

Nobusawa, E., Aoyama, T., Kato, H., Suzuki, Y., Tateno, Y., and Nakajima, K. (1991). Comparison of complete amino acid sequences and receptor-binding properties among 13 serotypes of hemagglutinins of influenza A viruses. Virology *182*, 475–485.

Osterhaus, A.D., Yang, H., Spijkers, H.E., Groen, J., Teppema, J.S., and van Steenis, G. (1985). The isolation and partial characterization of a highly pathogenic herpesvirus from the harbor seal (Phoca vitulina). Arch. Virol. *86*, 239–251.

PAHO (2004). Avian influenza virus A (H10N7) circulating among humans in Egypt. EID Wkly. Update *2*. https://www.paho.org/en/documents/avian-influenza-virus-h10n7-circulating-among-humans-egypt-vol-2-no-18-7-may-2004.

Pappas, C., Viswanathan, K., Chandrasekaran, A., Raman, R., Katz, J.M., Sasisekharan, R., and Tumpey, T.M. (2010). Receptor specificity and transmission of H2N2 subtype viruses isolated from the pandemic of 1957. PLoS One *5*, e11158.

Peng, W., de Vries, R.P., Grant, O.C., Thompson, A.J., McBride, R., Tsogtbaatar, B., Lee, P.S., Razi, N., Wilson, I.A., Woods, R.J., and Paulson, J.C. (2017). Recent H3N2 viruses have evolved specificity for extended, branched human-type receptors, conferring potential for increased avidity. Cell Host Microbe *21*, 23–34.

Russell, R.J., Gamblin, S.J., Haire, L.F., Stevens, D.J., Xiao, B., Ha, Y., and Skehel, J.J. (2004). H1 and H7 influenza haemagglutinin structures extend a structural classification of haemagglutinin subtypes. Virology *325*, 287–296.

Russier, M., Yang, G., Marinova-Petkova, A., Vogel, P., Kaplan, B.S., Webby, R.J., and Russell, C.J. (2017). H1N1 influenza viruses varying widely in hemagglutinin stability transmit efficiently from swine to swine and to ferrets. PLoS Pathog. *13*, e1006276.

Russier, M., Yang, G., Rehg, J.E., Wong, S.S., Mostafa, H.H., Fabrizio, T.P., Barman, S., Krauss, S., Webster, R.G., Webby, R.J., and Russell, C.J. (2016). Molecular requirements for a pandemic influenza virus: an acid-stable hemagglutinin protein. Proc. Natl. Acad. Sci. USA *113*, 1636–1641.

Schrauwen, E.J., Richard, M., Burke, D.F., Rimmelzwaan, G.F., Herfst, S., and Fouchier, R.A. (2016). Amino acid substitutions that affect receptor binding and stability of the hemagglutinin of influenza A/H7N9 virus. J. Virol. *90*, 3794–3799.

Short, K.R., Richard, M., Verhagen, J.H., van Riel, D., Schrauwen, E.J., van den Brand, J.M., Mänz, B., Bodewes, R., and Herfst, S. (2015). One health, multiple challenges: the inter-species transmission of influenza A virus. One Health *1*, 1–13.

Skehel, J.J., and Schild, G.C. (1971). The polypeptide composition of influenza A viruses. Virology *44*, 396–408.

Skehel, J.J., and Wiley, D.C. (2000). Receptor binding and membrane fusion in virus entry: the influenza hemagglutinin. Annu. Rev. Biochem. *69*, 531–569.

Tzarum, N., de Vries, R.P., Peng, W., Thompson, A.J., Bouwman, K.M., McBride, R., Yu, W., Zhu, X., Verheije, M.H., Paulson, J.C., and Wilson, I.A. (2017a). The 150-loop restricts the host specificity of human H10N8 influenza virus. Cell Rep. *19*, 235–245.

Tzarum, N., McBride, R., Nycholat, C.M., Peng, W., Paulson, J.C., and Wilson, I.A. (2017b). Unique structural features of influenza virus H15 hemagglutinin. J. Virol. *91*, e00046–17.

Vachieri, S.G., Xiong, X., Collins, P.J., Walker, P.A., Martin, S.R., Haire, L.F., Zhang, Y., McCauley, J.W., Gamblin, S.J., and Skehel, J.J. (2014). Receptor binding by H10 influenza viruses. Nature *511*, 475–477.

Wang, N., Zou, W., Yang, Y., Guo, X., Hua, Y., Zhang, Q., Zhao, Z., and Jin, M. (2012). Complete genome sequence of an H10N5 avian influenza virus isolated from pigs in central China. J. Virol. *86*, 13865–13866.

Watanabe, T., Zhong, G., Russell, C.A., Nakajima, N., Hatta, M., Hanson, A., McBride, R., Burke, D.F., Takahashi, K., Fukuyama, S., et al. (2014). Circulating avian influenza viruses closely related to the 1918 virus have pandemic potential. Cell Host Microbe *15*, 692–705.

Westgeest, K.B., Bestebroer, T.M., Spronken, M.I., Gao, J., Couzens, L., Osterhaus, A.D., Eichelberger, M., Fouchier, R.A., and de Graaf, M. (2015). Optimization of an enzyme-linked lectin assay suitable for rapid antigenic characterization of the neuraminidase of human influenza A(H3N2) viruses. J. Virol. Methods *217*, 55–63.

WHO. (2002). WHO Manual on Animal Influenza Diagnosis and Surveillance (World Health Organization). https://apps.who.int/iris/bitstream/handle/10665/68026/WHO_CDS_CSR_NCS_2002.5.pdf?sequence=1&isAllowed=y.

Xiong, X., Coombs, P.J., Martin, S.R., Liu, J., Xiao, H., McCauley, J.W., Locher, K., Walker, P.A., Collins, P.J., Kawaoka, Y., et al. (2013a). Receptor binding by a ferret-transmissible H5 avian influenza virus. Nature *497*, 392–396.

Xiong, X., Martin, S.R., Haire, L.F., Wharton, S.A., Daniels, R.S., Bennett, M.S., McCauley, J.W., Collins, P.J., Walker, P.A., Skehel, J.J., and Gamblin, S.J. (2013b). Receptor binding by an H7N9 influenza virus from humans. Nature *499*, 496–499.

Yang, H., Chen, L.M., Carney, P.J., Donis, R.O., and Stevens, J. (2010). Structures of receptor complexes of a North American H7N2 influenza hemagglutinin with a loop deletion in the receptor binding site. PLoS Pathog. *6*, e1001081.

Zhang, H., de Vries, R.P., Tzarum, N., Zhu, X., Yu, W., McBride, R., Paulson, J.C., and Wilson, I.A. (2015). A human-infecting H10N8 influenza virus retains a strong preference for avian-type receptors. Cell Host Microbe *17*, 377–384.

Zhang, T., Bi, Y., Tian, H., Li, X., Liu, D., Wu, Y., Jin, T., Wang, Y., Chen, Q., Chen, Z., et al. (2014). Human infection with influenza virus A(H10N8) from live poultry markets, China, 2014. Emerg. Infect. Dis. *20*, 2076–2079.

Zohari, S., Neimanis, A., Härkönen, T., Moraeus, C., and Valarcher, J.F. (2014). Avian influenza A(H10N7) virus involvement in mass mortality of harbour seals (Phoca vitulina) in Sweden, March through October 2014. EURO Surveill. *19*, 20967.

Please cite this article in press as: Herfst et al., Hemagglutinin Traits Determine Transmission of Avian A/H10N7 Influenza Virus between Mammals, Cell Host & Microbe (2020), https://doi.org/10.1016/j.chom.2020.08.011

STAR★METHODS

KEY RESOURCES TABLE

REAGENT or RESOURCE	SOURCE	IDENTIFIER
Antibodies		
NP monoclonal antibody (IgG2a, clone Hb65)	ATCC	Cat# H16L104R5
goat-anti-mouse Ig FITC	BD biosciences, USA	Cat# 349031
Bacterial and Virus Strains		
Influenza virus: H10N7 A/harbour seal/NL/PV14-221_TS/2015	Bodewes et al., 2016	N/A
Influenza virus: H10N7 A/harbor seal/S1047_14_L/Germany/2014	Bodewes et al., 2016	N/A
Influenza virus: H10N7 A/mallard/NL/1/2014	This paper	N/A
Influenza virus: H10N7 A/Mallard/Sweden/51/2002	This paper	N/A
Influenza virus: H10N7 A/harbor seal/S1047_14_L/Germany/2014 Q226L mutant	This paper	N/A
Influenza virus: H10N7 A/harbor seal/S1047_14_L/Germany/2014 Q226L, G228S mutant	This paper	N/A
Influenza virus: H10N7 A/harbor seal/S1047_14_L/Germany/2014 Q226L,Δ228 mutant	This paper	N/A
Influenza virus: H10N7 A/mallard/NL/1/2014 Q226L mutant	This paper	N/A
Biological Samples		
Turkey red blood cells	In house	N/A
Chemicals, Peptides, and Recombinant Proteins		
EMEM with EBBS	Lonza	Cat# BESP069F
Penicillin-Streptomycin	Lonza	Cat# 17-603E
L-Glutamine (200 mM)	Lonza	Cat# 17-605F
sodium bicarbonate	Lonza	Cat#: 17-613E
1M HEPES	Lonza	Cat#: 17-737E
Non-essential amino acids (100x)	Lonza	Cat#: 13-114E
TPCK-treated trypsin	Sigma	T1426-1G
Vibrio cholerae neuraminidase (VCNA)	In house	N/A
Beta-propiolactone	Sigma-Aldrich	Cat# P5648
2x EMEM	Lonza	Cat#:BE12-668F
Avicel RC-591	IMCD Benelux BV	RC-591
Phosphate-buffered saline (PBS)	Oxoid	X6571D
OPD substrate	Sigma–Aldrich	P8287-50TAB
fetuin	Sigma-Aldrich	F3385-1G
Nunc-Immuno™ MicroWell™ 96 well solid plates	Sanbio, Uden, The Netherlands	442404
PNA-HRPO	Sigma-Aldrich	L7759-1MG
Xtremegene transfection reagent	Roche	06366546001
Giemsa	Merck Millipore	1092040500
0.05% Trypsin-EDTA (1x)	Gibco	Cat# 25300-054
6'SLN	Dextra Laboratories Ltd., Reading, UK	Cat#SLN306

(*Continued on next page*)

Please cite this article in press as: Herfst et al., Hemagglutinin Traits Determine Transmission of Avian A/H10N7 Influenza Virus between Mammals, Cell Host & Microbe (2020), https://doi.org/10.1016/j.chom.2020.08.011

Continued

REAGENT or RESOURCE	SOURCE	IDENTIFIER
3'SLN	Dextra Laboratories Ltd., Reading, UK	Cat#SLN302
6'SLN-PAA	Lectinity Holdings, Moscow, Russia	Cat#0997-BP
3'SLN-PAA	Lectinity Holdings, Moscow, Russia	Cat#0036-BP
Oseltamivir	Kind gift from Roche, Welwyn Garden City, UK	N/A
Zanamivir	Kind gift from GSK, Stevenage, UK	N/A
Trypsin	Sigma	Cat#T1426
H10sealG HA	This paper	N/A
H10sealG Q226L HA	This paper	N/A
H10sealG Q226L,G228S HA	This paper	N/A
H10sealG Q226L, Δ228 HA	This paper	N/A
H10sealNL HA	This paper	N/A
Critical Commercial Assays		
QuikChange multi-site-directed mutagenesis kit	Agilent	Cat# 200514
Dual-Glo Luciferase Assay System	Promega	Cat# E2920
Deposited Data		
H10sealG Q226L, Δ228 HA (apo) structure	This paper	PDB: 6TJW
The structure of H10sealG Q226L, Δ228 HA-3'SLN complex	This paper	PDB: 6TXO
The structure of H10sealG Q226L, Δ228 HA-6'SLN complex	This paper	PDB: 6TVT
H10sealG Q226L HA (apo) structure	This paper	PDB: 6TVR
The structure of H10sealG Q226L HA-3'SLN complex	This paper	PDB: 6TVS
The structure of H10sealG Q226L HA-6'SLN complex	This paper	PDB: 6TWV
H10sealNL HA (apo) structure	This paper	PDB: 6TVC
The structure of H10sealNL HA-3'SLN complex	This paper	PDB: 6TVA
The structure of H10sealNL HA-6'SLN complex	This paper	PDB: 6TVB
H10sealG Q226L, G228S HA (apo) structure	This paper	PDB: 6TWH
The structure of H10sealG Q226L, G228S HA-3'SLN complex	This paper	PDB: 6TWI
The structure of H10sealG Q226L, G228S HA-6'SLN complex	This paper	PDB: 6TY1
The structure of H10sealG Q226L, G228S HA- EDTA complex	This paper	PDB: 6TWS
H10sealG HA (apo) structure	This paper	PDB: 6TJY
The structure of H10sealG HA-3'SLN complex	This paper	PDB: 6TVD
Experimental Models: Cell Lines		
Human: HEK 293T cells	N/A	N/A
Canine: MDCK II cells	ATCC	Cat# CCL-34
Q10 Seal (Phoca Vitulina) kidney cells	Osterhaus et al., 1995)	N/A
Embryonated chicken eggs	Drost	N/A
Spodoptera frugiperda: Cell line Sf9	Thermo Fisher Scientific	Cat#12659017
Experimental Models: Organisms/Strains		
Ferret (Mustela putorius furo)	Euroferret	N/A

(*Continued on next page*)

Please cite this article in press as: Herfst et al., Hemagglutinin Traits Determine Transmission of Avian A/H10N7 Influenza Virus between Mammals, Cell Host & Microbe (2020), https://doi.org/10.1016/j.chom.2020.08.011

Continued

REAGENT or RESOURCE	SOURCE	IDENTIFIER
Recombinant DNA		
Plasmid: pHW2000 (modified version)	(Chutinimitkul et al., 2010)	N/A
Plasmid: pFB-H10sealG HA	Thermo Scientific	N/A
Plasmid: pFB-H10sealG Q226L HA	Thermo Scientific	N/A
Plasmid: pFB-H10sealG Q226L, Δ228 HA	Thermo Scientific	N/A
Plasmid: pFB-H10sealG Q226L, G228S HA	Thermo Scientific	N/A
Plasmid: pFB-H10sealNL HA	Thermo Scientific	N/A
Software and Algorithms		
ImageQuant TL Software	GE Healthcare Life Sciences	N/A
Q11 iMOSFLM	Battye et al., 2011	N/A
Q12 Aimless	Evans and Murshudov, 2013	N/A
Q13 Pointless	Evans, 2006	N/A
The CCP4 suite	Collaborative Computational Project, 1994	N/A
Phenix	Adams et al., 2010	N/A
Other		
Minigenome assay	de Wit et al., 2010	N/A
Sialoside glycan microarray	This paper and (Peng et al., 2017)	N/A

RESOURCE AVAILABILITY

Lead Contact

Further information and requests for resources and reagents should be directed to and will be fulfilled by the lead contact, Ron Fouchier (r.fouchier@erasmusmc.nl).

Materials availability

All unique reagents generated in this study are available from the Lead Contact with a completed Materials Transfer Agreement.

Data and code availability

All datasets for glycan microarray experiments are included in the supplement according to the MIRAGE consortium format (Table S4, supplementary glycan microarray document). These datasets have not been uploaded to a public repository since, at present, such a resource does not exist. Structural data have been deposited with the Protein Data Bank under accession codes 6TJW, 6TXO, 6TVT, 6TVR, 6TVS, 6TWV, 6TVC, 6TVA, 6TVB, 6TWH, 6TWI, 6TY1, 6TWS, 6TJY, 6TVD, 6TVF.

EXPERIMENTAL MODEL AND SUBJECT DETAILS

Experimental Animals

Forty female ferrets (*Mustela putorius furo*), 12- to 24- month old, sero-negative for prototype A/H1, A/H3 and A/H5 influenza A viruses and Aleutian Disease Virus, were obtained from an accredited ferret breeder. All animals were microchipped and received hormonal treatment to prevent estrus. Ferrets were housed with a 12 h light/dark cycle and allowed access to diet and water. The experimental set-up was specifically designed to allow transmission experiments to be conducted in negatively pressurized isolator cages (1.6m x 1m x 1m) in the ABSL3+ facility. During the experiment the ferrets are housed in clear Perspex cages, in which each inoculated animal was housed individually next to a naive ferret. Each ferret cage was 30 cm x 30 cm x 55 cm (W x H x L) and the two cages were separated by two stainless steel grids (1), with a grid size of 0.5 cm^2,10 cm apart. Experiments were performed in strict compliance with European guidelines (EU Directive on Animal Testing 86/609/EEC) and Dutch legislation (Experiments on Animals Act, 1997). An independent animal experimentation ethical review committee (Dutch Stichting Dier Experimenten Commissie Consult) approved all animal studies.

METHOD DETAILS

Biocontainment

All experiments involving the seal A/H10N7 viruses were conducted at enhanced animal biosafety level 3 (ABSL3+). The ABSL3+ facility of Erasmus MC consists of a negative pressurized (-30 Pa) laboratory in which all *in vivo* and *in vitro* experimental work is

Please cite this article in press as: Herfst et al., Hemagglutinin Traits Determine Transmission of Avian A/H10N7 Influenza Virus between Mammals, Cell Host & Microbe (2020), https://doi.org/10.1016/j.chom.2020.08.011

carried out in class 3 isolators or class 3 biosafety cabinets, which are also negative pressurized (< -200 Pa). Although the laboratory is considered 'clean' because all experiments are conducted in closed class 3 cabinets and isolators, special personal protective equipment, including laboratory suits, gloves and FFP3 facemasks is used. Air released from the class 3 units is filtered by High Efficiency Particulate Air (HEPA) filters and then leaves the facility via a second set of HEPA filters. Only authorized personnel that received the appropriate training can access the ABSL3+ facility. All personnel working in the facility is vaccinated against seasonal and A/H5N1 influenza viruses. For animal handling in the facilities, personnel always work in pairs. The facility is secured by procedures recognized as appropriate by the institutional biosafety officers and facility management at Erasmus MC and Dutch and United States government inspectors. Antiviral drugs (oseltamivir and zanamivir) and personnel isolation facilities are directly available to further mitigate risks upon incidents. All experiments described in this manuscript were performed with naturally occurring viruses, and therefor this research does not fall under the pause on gain-of-function research.

Viruses

Influenza viruses A/harbour seal/NL/PV14-221_TS/2015 (H10sealNL) and A/harbor seal/S1047_14_L/Germany/2014 (H10sealG) were propagated in MDCK cells (Bodewes et al., 2016). Influenza virus A/mallard/NL/1/2014 (H10mall) was propagated in embryonated chicken eggs followed by one passage in MDCK cells. All eight gene segments were amplified by reverse transcription polymerase chain reaction and cloned in a modified version of the bidirectional reverse genetics plasmid pHW2000 (Chutinimitkul et al., 2010; de Wit et al., 2004). Substitutions of interest were introduced by reverse genetics using the QuikChange multi-site-directed mutagenesis kit (Agilent Netherlands, Amstelveen, Netherlands) according to the instructions of the manufacturer. Recombinant viruses were produced upon transfection of 293T cells and virus stocks were propagated in MDCK cells or embryonated chicken eggs (Drost, Loosdrecht, The Netherlands) and titrated in MDCK cells. For binding assays and stability assays, reassortant viruses consisting of seven gene segments of influenza virus A/PR/8/34 and the HA segment of interest were produced using a previously described reverse genetics system for influenza virus A/PR/8/34 (de Wit et al., 2004).

Virus Titration in MDCK Cells

Virus titers were determined by end-point titration in MDCK cells. MDCK cells were inoculated with tenfold serial dilutions of virus stocks, nose swabs, or throat swabs. Cells were washed with PBS one hour after inoculation and cultured in 200μl of infection media, consisting of Eagle's Minimum Essential Medium (EMEM) supplemented with 100 U/ml penicillin, 100 μg/ml streptomycin, 2 mM glutamine, 1.5 mg/ml sodium bicarbonate, 10 mM HEPES (4-(2-hydroxyethyl)-1-piperazineethanesulfonic acid), non-essential amino acids, and 20 μg/ml N-tosyl-L-phenylalanine chloromethyl ketone (TPCK) treated trypsin (Sigma). Three days after inoculation, supernatants of infected cell cultures were tested for agglutinating activity using turkey red blood cells (TRBCs) as an indicator of virus replication in the cells. Infectious virus titers were calculated from 4 replicates (nose swabs, and throat swabs) or 10 replicates (virus stocks) by the method of Spearman-Karber.

Transmission of A/H10N7 Virus via Aerosols or Respiratory Droplets in the Ferret Model

We chose the ferret (*Mustela putorius furo*) as the animal model for our studies. Ferrets have been used in influenza research since 1933 because they are susceptible to infection with human and avian influenza viruses. After infection with human influenza A virus, ferrets develop respiratory disease and lung pathology similar to that observed in humans. Ferrets can also transmit human influenza viruses via the air to other ferrets that serve as sentinels with or without direct contact. Aerosol or respiratory droplet transmission experiments were performed as described previously (Herfst et al., 2012; Munster et al., 2009). In short, seronegative female adult ferrets were inoculated intranasally with 10^6 50% Tissue Culture Infectious Dose ($TCID_{50}$) of virus by applying 250 μl of virus suspension to each nostril. Each ferret was then placed in a transmission cage. One day after inoculation, one naïve ferret was placed opposite to each inoculated ferret. Each transmission pair was housed in a separate transmission cage designed to prevent direct contact between the inoculated and naïve ferrets but allowing airflow from the inoculated to the naïve ferret. Nose and throat swabs were collected on 1, 3, 5, and 7 days post inoculation (dpi) for inoculated ferrets and on 1, 3, 5, 7, and 9 days post exposure (dpe) for the naïve ferrets. Virus titers in swabs were determined by end-point titration in MDCK cells. All animals were humanely euthanized at 14 dpi/dpe.

Serology

The presence of antibodies elicited against the tested viruses were confirmed by hemagglutination inhibition (HI) assay using standard procedures (WHO, 2002). Briefly, ferret antisera were prepared following intranasal inoculation, from blood collected 14 days later. Antisera were pre-treated overnight with receptor destroying enzyme *Vibrio cholerae* neuraminidase (VCNA) at 37°C, and incubated at 56°C for 1h the next day. Two-fold serial dilutions of the antisera, starting at a 1:20 dilution, were mixed with 25 μl of a virus stock containing 4 hemagglutinating units and were incubated at 37°C for 30 minutes. Subsequently, 25 μl 1% TRBCs was added and the mixture was incubated at 4°C for 1h. HI was read and was expressed as the reciprocal value of the highest dilution of the serum that completely inhibited agglutination of virus and erythrocytes.

Purification of HAs

The ecto domains of all A/H10 seal HAs were cloned into a pFastBac1 vector. This vector was edited for HA ectodomain expression, which contained a polyhedrin signal peptide at the N-terminal of HA and a tobacco etch virus cleavage site, a foldon for trimerization

Please cite this article in press as: Herfst et al., Hemagglutinin Traits Determine Transmission of Avian A/H10N7 Influenza Virus between Mammals, Cell Host & Microbe (2020), https://doi.org/10.1016/j.chom.2020.08.011

and an octa-histidine tag at the C-terminus of HA. All A/H10 seal HAs were expressed in Sf9 cells and purified by a combination of Co-NTA (Co^{3+} complex with nitrilotriacetic acid) chromatography, trypsin digestion and gel filtration chromatography (Lin et al., 2012).

Crystallization

Purified H10 seal HAs were concentrated to 10 mg/ml for crystallization. H10sealG was crystallized in 2%-4% PEG6000, 0.1M HEPES pH7.0 and 8% PEG6000, 22% ethylene glycerol, 0.1M HEPES pH 7.5 was used as a cryoprotectant for flash freezing in liquid nitrogen. H10sealG Q226L was crystallized in 4% PEG3350, 0.1M HEPES pH 7.5 and 15%PEG3350, 20% ethylene glycol, 0.1M HEPES pH7.5 was applied as a cryoprotectant for flash freezing in liquid nitrogen. H10sealG Q226L,Δ228 mutant crystals were grown in 10% PEG6000, 0.1M bicine pH9.0 and flash freezing in liquid nitrogen with the cryoprotectant 12% PEG6000, 22% ethylene glycol, 0.1 M bicine pH9.0. H10sealG Q226L/G228S crystals were grown in 6% PEG3350, 0.1 M MES pH 6.5 and flash freezing in liquid nitrogen with a cryoprotectant 15% PEG3350, 20% ethylene glycol, 0.1 M HEPES pH 7.5. H10sealNL crystals were grown in 26%-31% PEG600, 0.1M HEPES pH7.5 or 0.1M tris pH8.0 and flash freezing in liquid nitrogen with a cryoprotectant 33% PEG600, 15% ethylene glycol, 0.1M HEPES pH7.5. Crystals were soaked for 3mins-6mins in 100mM 3'-sialyl-N-acetyllactosamine (SLN) or 6'-SLN in cryobuffer. All the data sets were collected at the Diamond Light Source, Harwell, Oxfordshire, UK. Diffraction datasets were processed using Xia2 DIALS, imosflm and scala (Collaborative Computational Project, 1994). Structures were solved by molecular replacement with Phaser and the coordinate file of A/H10 A/Jiangxi-Donghu/346/2013 HA (Protein Data Bank [PDB] entry 4D00) was used as a searching model (Vachieri et al., 2014). The structures were manually built in coot (Emsley and Cowtan, 2004) and refined by using Refmac5 (Collaborative Computational Project, 1994) and Phenix (Adams et al., 2010).

Virus Preparation for Biolayer Interferometry

All the A/H10N7 seal influenza viruses were inoculated in embryonated hens' eggs for virus propagation. The allantoic fluid from infected eggs was harvested after incubation of the infected eggs for 72 hrs and all the viruses were obtained from the allantoic fluid by centrifugation and were purified by sucrose gradient untracentrifugation (Skehel and Schild, 1971). The concentrations of purified viruses were determined by combined methods including gel quantification and ELISA (enzyme-linked immunosorbent assay) (Lin et al., 2012).

Biolayer Interferometry

Virus binding to defined receptor analogues was measured on an Octet RED biolayer interferometer (Pall ForteBio Corp., Menlo Park, CA, USA). Biotinylated α2,3- and α2,6-linked SLN were purchased from Lectinity Holding, Inc. (Moscow, Russia). These were approximately 30 kDa polymers containing 20% mol. sugar and 5% mol. biotin linked to a polyacrylamide backbone. The polymers were immobilized on streptavidin biosensors (Pall ForteBio Corp., Menlo Park, CA, USA) at concentrations ranging from 0.01 to 1.5 μg/ml. The relative sugar loading (RSL) of the biosensor was calculated from the amplitude of the response at the end of the 5-10 minute loading step. The maximum response at complete saturation was ~ 0.6 nm.

Binding of viruses (at 1nM) was measured at 25°C in a 30-50 minute association step. The buffer was 10 mM HEPES (pH 7.4), 150 mM NaCl, 2 mM $CaCl_2$ and 0.005% Tween-20. All solutions also contained 10 μM oseltamivir carboxylate (Roche, Welwyn Garden City, U.K.) and 10 μM zanamivir (GSK, Stevenage, U.K.) to prevent cleavage of the receptor analogues by the viral neuraminidase.

The (relative) amount of virus bound to the biosensor at different relative sugar loadings was calculated from the amplitude of the response at the end of the association step. The measured amplitudes were normalized by dividing by the maximum response (typically 5-6 nm) and the normalized response was plotted as a function of the relative sugar loading. The normalized virus binding response curves report the fractional saturation of the sensor surface (f) and smooth lines through the curves were generated by fitting the data to a simple variant of the Hill equation:

$$f = \frac{[RSL]^n}{[RSL_{0.5}]^n + [RSL]^n}$$

where RSL is the relative sugar loading, $RSL_{0.5}$ is the relative sugar loading at half saturation (f = 0.5), and n is a Hill coefficient.

Virus Preparation for Glycan Array

All viruses were inoculated in embryonated hens' eggs for virus propagation. The allantoic fluid from infected eggs was harvested after incubation of the infected eggs for 72 hrs and all the viruses were obtained from the allantoic fluid, inactivated with beta-propiolactone, and concentrated and purified by sucrose gradient ultracentrifugation. The HA titer was determined and samples were stored at -80°C.

Glycan Array Fabrication

Glycan arrays were prepared as previously described (Peng et al., 2017). Briefly, a library of asialo and sialylated glycans bearing a reducing-end amine were dissolved to 100uM concentration in printing buffer (150mM sodium phosphate + 0.005% Tween-20, pH 8.2) and aliquoted into 384-well microtiter plates. Using a MicroGrid II (Digilab) microarray printing robot, equipped with SMP3 microarray pins (Telechem), 6 replicate spots of each glycan were immobilized onto NHS-activated glass microscope slides (SlideH,

Schott). Following printing, slides were blocked to quench remaining NHS chemistry in blocking buffer (50mM ethanolamine in 50mM borate buffer, pH 9.4) and stored at -20C until used.

Virus Labeling and Binding Assays

Viruses were directly labeled with a biotin handle as previously described (Watanabe et al., 2014). Labeled viruses were diluted to 256 hemagglutinating units (HAU) in 1X PBS and applied directly to the slide surface for 1h. Following the initial incubation, arrays were washed, by dipping 3 times in 1X PBS and again 3 times in 1X PBS. Washed arrays were incubated with 2ug/mL streptavidin-AlexaFluor555 (LifeTechnologies) in 1X PBS, for 1h. Following detection, arrays were washed sequentially, by dipping, 3 times in 1X PBS, 3 times in 1X PBS and, finally, 3 times in deionized H2O. Washed arrays were dried by centrifugation and immediately scanned for AlexaFluor555 signal on an Innoscan 1100AL (Innopsys) confocal microarray scanner. Signal intensity from scanned arrays was collected using Mapix (Innopsys). Signal intensity was calculated for the mean signal intensity of 4 replicate spots for each printed glycan and graphed using Excel (Microsoft).

CD Measurements

Far-ultraviolet (UV) circular dichroism (CD) spectra were recorded on a Jasco J-815 spectropolarimeter fitted with a cell holder thermostatted by a CDF-426S Peltier unit. All CD measurements were made in 10mM HEPES, 150mM NaCl with and without 2 mM $CaCl_2$ using fused silica cuvettes with 1-mm path length (Hellma, Jena, Germany). CD intensities are presented as the CD absorption coefficient calculated on a mean residue weight basis ($\Delta\varepsilon$MRW).

Thermal unfolding curves were obtained by monitoring the ellipticity at 222 nm using 1- or 2-mm path length cuvettes and a heating rate of 1 °C/min over the temperature range 20 to 90 °C. The transition mid-point temperature was obtained by fitting to a modified Gibbs-Helmholtz equation using in-house software as described elsewhere [1].

Trp Fluorescence Assay

0.25 mg/ml HA protein in the presence or absence of 2 mM calcium was denatured using different concentrations of urea (1-10 M) at room temperature overnight except HAs with high stability that required higher temperature (30°C) to be unfolded. Fluorescence spectra were recorded on a Jasco FP-6300 spectrofluorometer. Each sample was placed into a 3 mm Cuvette and excited using 280 nm UV light and the emission spectra (from 300 to 450 nm) were obtained. The optical signals at 341nm from HAs in different concentrations of urea had maximum variation, so they were chosen to be plotted against the corresponding urea concentrations for data analysis.

Calcium Binding Assays

Macroscopic calcium binding constants (K_1-K_3) were determined from calcium titrations performed in the presence of the chromophoric calcium chelator, 5,5'-Br_2BAPTA (5,5'-dibromo-1,2-bis(2-aminophenoxy)ethane-N,N,N',N'-tetraacetic acid), using a method described by Linse et al. [2].

Measurements were performed at 20 °C in calcium free buffer (Chelex-100 treated 10 mM HEPES, 100 mM NaCl, pH 8); under these conditions, the calcium binding constant of 5,5'-Br_2-BAPTA was determined to be 5.7 x 10^5 M^{-1}. The values for the individual binding constants (K1-K3) were obtained from least-squares fits directly to the experimentally observed titration curves using in-house software.

pH Dependent Proteolysis Experiment

0.2 mg/ml HA in PBS buffer was adjusted to pH ranging from 6.84 to 4.98 using 150 mM citrate buffer, pH 3.5, and incubated at room temperature for 10 min. The pH was then adjusted to 7.5 using 1 M tris buffer, pH 8.0. The samples were treated with trypsin (10μg/ml) at 37°C for 10 min and then treated with trypsin inhibitor to stop all the reactions.

Minigenome Assay

A model vRNA, consisting of the firefly luciferase open reading frame flanked by the noncoding regions (NCRs) of segment 8 of influenza A virus, under the control of a T7 RNA polymerase promoter was used for minigenome assays (de Wit et al., 2010). The reporter plasmid (0.5 μg) was transfected into 293T cells in 6-well plates, along with 0.5 μg of each of the pHW2000 plasmids encoding PB2, PB1, PA, and NP; 1 μg of pAR3132 expressing T7 RNA polymerase (Dunn et al., 1988); and 0.02 μg of the *Renilla* luciferase expression plasmid pRL (Promega, Leiden, Netherlands) as an internal control. Forty-two hours after transfection, luminescence was measured using a Dual-Glo Luciferase Assay System (Promega) according to the instructions of the manufacturer in a TECAN Infinite F200 machine (Tecan Benelux bv, Giessen, Netherlands). Relative light units (RLU) were calculated as the ratio of firefly and *Renilla* luciferase luminescence.

Plaque Assay

The assay was performed as described (Matrosovich et al., 2006). In brief, MDCK cells (10^6 per well) were seeded in a 6 well plate to reach 90% confluency the next day. Recombinant virus supernatants were diluted and 100 μl of the selected dilution, to obtain a plaque density of ~20, was added to each well. After incubation for one hour at 37 °C and 5% CO2 cells were washed with PBS once and 2 ml of an overlay containing 2x EMEM (Lonza) and avicel (FMC BioPolymer, Newark, US) in a 1:1 ratio was added. Plates

Please cite this article in press as: Herfst et al., Hemagglutinin Traits Determine Transmission of Avian A/H10N7 Influenza Virus between Mammals, Cell Host & Microbe (2020), https://doi.org/10.1016/j.chom.2020.08.011

were incubated at 37 °C and 5% CO2. After 40 h, cells were washed with PBS twice and 1 ml of 80% acetone was added. Plates were incubated at -20 °C overnight and virus infection was determined by NP antibody staining. Briefly, NP monoclonal antibody (IgG2a, clone Hb65, American Type Culture Collection, Wesel, Germany) and goat-anti-mouse Ig FITC (BD biosciences, USA) antibody were used to detect NP positive cells. Digital images were taken using ImageQuant TL software (GE Healthcare Life Sciences). The plaque sizes of some viruses were too small to analyze with the software.

Replication Kinetics in Seal Cells

Seal (*Phoca vitulina*) kidney cells (Osterhaus et al., 1985) were inoculated with 0.1 $TCID_{50}$/cell of virus. Cells were washed with PBS one hour after inoculation and cultured in 200μl of infection media, consisting of EMEM supplemented with 100 U/ml penicillin, 100 μg/ml streptomycin, 2 mM glutamine, 1.5 mg/ml sodium bicarbonate, 10 mM HEPES, non-essential amino acids, and 20 μg/ml TPCK treated trypsin (Lonza). Supernatant samples were harvested 6, 12, 24, 48 and 72 h later. Virus titers were determined by end-point titration in MDCK cells.

Enzyme-Linked Lectin Assay

The enzyme-linked lectin assay (ELLA) was performed as described previously to measure neuraminidase activity (Westgeest et al., 2015). In brief, fetuin (25 ug/ml) was used to coat Nunc-Immuno™ MicroWell™ 96 well solid plates (100 μl/well; Sanbio, Uden, The Netherlands) at 4 °C for at least 24 h. Twofold serial dilutions of reassortant viruses consisting of seven gene segments of influenza virus A/PR/8/34 and the N7 NA segment of interest were added to duplicate fetuin-coated plates. Plates were sealed and incubated at 37 °C for 16–18 h. The plates were washed and 100 μl/well of horseradish peroxidase-conjugated peanut agglutinin lectin (PNA-HRPO, Sigma–Aldrich) was added. Plates were incubated at room temperature for 2 h. *O*-Phenylenediamine dihydrochloride (OPD, Sigma–Aldrich) substrate was freshly prepared following the manufacturer's instruction and added to the plate (100 μl/well). The reaction was stopped after 10 min by the addition of stop solution (0.5 M H_2SO_4, 100 μl/well). The plates were read at 490 nm (OD_{490}) for 0.25 s using an Infinite 200 96-well plate reader (Tecan, Giessen, The Netherlands). Next the NA activity was plotted against the antigen dilutions.

Fusion (Acid Stability) Assay

Membrane fusion was tested as previously described (Herfst et al., 2008) in a cell content mixing (CM) assay in which two 10 cm cultures dishes containing Vero-118 cells were transfected with 5 μg of pCAGGS-HA and 5 μg of pEGFP-N1 (as transfection control) using Xtremegene transfection reagent (Roche). One day after transfection, cell populations were harvested using trypsin-EDTA (Ethylenediaminetetraacetic acid), and plated in a 12-well plate format. The next morning, cells were exposed to PBS at different pH for 10 minutes. Cells were fixed 24 hours after the pH-pulse using 70% ice-cold acetone, washed and stained using a 20% Giemsa mixture for microscopy (Merck Millipore, Darmstadt, Germany).

QUANTIFICATION AND STATISTICAL ANALYSIS

For the ferret transmission experiments, the Fisher's Exact Test ($p = 0.04$) was used for the comparison of transmissibility of H10sealNL virus (transmission in 6 out of 8 ferret pairs) and H10mall (transmission in 1 out of 8 transmission pairs), Figures 1 and S1. Fluorescence intensities recorded using Mapix (Innopsys) for glycan microarray experiments in Figure 2 were quantified via measurement of mean intensity minus mean background of the four median out of six total replicate spots. Data presented is the average of these four replicates with standard error. Statistical analysis is not applied. The statistical analysis to validate all the crystal structures is included in Table S2 (Crystallographic data and refinement statistics).

Cell Host & Microbe, Volume *28*

Supplemental Information

Hemagglutinin Traits Determine Transmission of Avian A/H10N7 Influenza Virus between Mammals

Sander Herfst, Jie Zhang, Mathilde Richard, Ryan McBride, Pascal Lexmond, Theo M. Bestebroer, Monique I.J. Spronken, Dennis de Meulder, Judith M. van den Brand, Miruna E. Rosu, Stephen R. Martin, Steve J. Gamblin, Xiaoli Xiong, Wenjie Peng, Rogier Bodewes, Erhard van der Vries, Albert D.M.E. Osterhaus, James C. Paulson, John J. Skehel, and Ron A.M. Fouchier

SUPPLEMENTAL TABLES

Table S1. Related to Figure 1**.** Amino acid differences between H10mall, H10sealG and H10sealNL.

PB2	H10mall	H10sealG	H10sealNL
AA position			
17	R	C	C
64	T	M	M
147	V	I	I
598	T	T	A
676	T	I	I

PB1	H10mall	H10sealG	H10sealNL
AA position			
14	A	V	V
62	G	R	R
76	D	N	N
94	F	S	S
119	M	V	V
154	G	S	G
273	V	I	I
453	A	S	S
577	K	R	R
687	Q	R	R
694	S	N	N
752	E	E	D

PA	H10mall	H10sealG	H10sealNL
AA position			
144	H	H	Q
192	R	H	H
196	R	K	K
277	S	A	A
405	S	C	C

HA	H10mall	H10sealG	H10sealNL
AA position			
91	E	K	K
103	A	V	V
122	S	N	N
171	T	A	A
210	Q	K	K
212	N	N	S
226	Q	Q/L	L
242	N	K	K
244	T	T	I
263	K	R	R
270	D	E	E
276	N	S	S
327	M	V	V
55 (HA_2)	L	I	I
57 (HA_2)	E	K	K
74 (HA_2)	E	D	D
158 (HA_2)	D	D	N
184 (HA_2)	D	N	N

NP	H10mall	H10sealG	H10sealNL
AA position			
52	Y	H	H
105	V	M	M
329	V	V	M
428	A	V	V

NA	H10mall	H10sealG	H10sealNL
AA position			
81	P	S	S
158	V	I	I
247	S	S	I
436	A	A	T

M2	H10mall	H10sealG	H10sealNL
AA position			
21	D	G	G
55	L	L	F

NS1	H10mall	H10sealG	H10sealNL
AA position			
55	E	E	K
81	I	V	V
94	T	I	T
126	R	K	K
171	D	Y	Y

Table S3. Related to Figure 7. Syncytium formation assay at a pH range of 4.8 to 5.9 (with intervals of 0.1 pH).

Hemagglutinin	Threshold pH for fusion	Stability change compared to wt HA[#]
A/Netherlands/213/2003 [A/H3]	5,4	
A/Indonesia/5/2005 [A/H5]	5,7	wt
A/Indonesia/5/2005 [A/H5] +160A/226L/228S	5,8	↓
A/Indonesia/5/2005 [A/H5] +110Y/160A/226L/228S	5,4	↑
A/Seal/Sweden/SVA1412040224-S/25634/2014 [A/H10]	5,5	
A/Seal/Sweden/SVA1412040224-SZ1847/2014 [A/H10]	5,3	
H10sealG	5,1	
A/Seal/Netherlands/PV336/2014 [A/H10]	5,4	
H10sealNL	5,2	
H10mall	5,5	
Substitutions in HAmall		
H10mall	**5,5**	**wt**
H10mall + E91K	5,5	-
H10mall + A103V	5,6	↓
H10mall + S122N	5,6	↓
H10mall + T171A	5,6	↓
H10mall + Q210K	5,7	↓
H10mall + N212S	5,5	-
H10mall + Q226L	**5,7**	↓
H10mall + N242K	5,6	↓
H10mall + T244I	**5,3**	↑
H10mall + K263R	5,5	-
H10mall + D270E	5,6	↓
H10mall + N276S	5,5	-
H10mall + M327V	5,5	-
H10mall + L55I (HA_2)	5,4	↑
H10mall + E57K (HA_2)	5,4	↑
H10mall + E74D (HA_2)	**5,3**	↑
H10mall + D158N (HA_2)	5,5	-
H10mall + D184N (HA_2)	5,5	-
H10mall + T244I/E74D (HA_2)	**5,1**	↑
H10mall + Q226L/T244I/E74D (HA_2)	**5,2**	↑
Substitutions introduced in HAsealNL		
H10sealNL	**5,2**	**wt**
H10sealNL + L226Q	**4,9**	↑
H10sealNL + I244T	**5,4**	↓
H10sealNL + D74E (HA_2)	**5,4**	↓
H10sealNL + I244T/D74E (HA_2)	**5,6**	↓
H10sealNL + L226Q/I244T/D74E (HA_2)	**5,5**	↓

Table S4. Related to Figure 2. Supplementary glycan microarray document, based on MIRAGE Guidelines (doi:10.3762/mirage.3).

Classification	Guidelines
1. Sample: Glycan Binding Sample	
Description of Sample	Recombinant hemagluttinin (HA) proteins originating from Influenza TypeA viruses. HA: Fig2 Fig2a - HAmall Fig2b - HA A/H10N2mall Fig2c - HAsealNL Fig2d - HAmall Q226L Fig2e - HAsealG Fig2f - HAsealG Q226L Fig2g - HAsealG Q226L, G228S Fig2h - HAsealG Q226L Δ228 Influenza viruses A/harbour seal/NL/PV14-221_TS/2015 (H10sealNL) and A/harbor seal/S1047_14_L/Germany/2014 (H10sealG) were propagated in MDCK cells (Bodewes et al., 2016). Influenza virus A/mallard/NL/1/2014 (H10mall) was propagated in embryonated chicken eggs followed by one passage in MDCK cells. All eight gene segments were amplified by reverse transcription polymerase chain reaction and cloned in a modified version of the bidirectional reverse genetics plasmid pHW2000 (Chutinimitkul et al., 2010; de Wit et al., 2004). Substitutions of interest were introduced by reverse genetics using the QuikChange multi-site-directed mutagenesis kit (Stratagene, Leusden, Netherlands) according to the instructions of the manufacturer. Recombinant viruses were produced upon transfection of 293T cells and virus stocks were propagated in MDCK cells or embryonated chicken eggs and titrated in MDCK cells. For binding assays and stability assays, reassortant viruses consisting of seven gene segments of influenza virus A/PR/8/34 and the HA segment of interest were produced using a previously described reverse genetics system for influenza virus A/PR/8/34 (de Wit et al., 2004).
Sample modifications	Viruses were directly labeled with a biotin handle as previously described (Cell Host Microbe. 2014 Jun 11;15(6):692-705. doi: 10.1016/j.chom.2014.05.006.PMID:24922572)
Assay protocol	Please see method section in the main text.
2. Glycan Library	
Glycan description for defined glycans	In-house sialoside array, consisting of 135 defined glycans. The synthesis of the contained glycans are described in Supplemental Experimental Procedures 5.Experimental Section. Peng et al., Glycobiology (2012) PMID: 22786570

Glycan description for undefined glycans	No glycans are undefined.
Glycan modifications	No modifications after initial synthesis were made.
3. Printing Surface; e.g., Microarray Slide	
Description of surface	NHS-ester functionalized hydro-polymer
Manufacturer	Schott SlideH (Applied Microarrays 1070936)
Custom preparation of surface	None
Non-covalent Immobilization	All glycans are terminated with primary amine linker (either natural amino acid or chemical linker) Xu et al. JVI (2012) PMID: 22072785
4. Arrayer (Printer)	
Description of Arrayer	MicroGrid II (Digilab)
Dispensing mechanism	Contact microarray pins (SMP3, ArrayIt)
Glycan deposition	Manufacturer estimation is 0.7nL per spot. However, actual delivery volume of each printed spot is not determined. Each glycan was “pre-spotted” 3 times on Poly-L-Lysine derivatized slides (made in-house) before being spotted on SlideH slides. Each array contains 6 replicate spots of each individual glycan.
Printing conditions	Glycans were diluted to 100uM in 150mM NaPO4 buffer, pH 8.4 + 0.005% Tween-20. 10uL of each glycan was transferred to a 384-well microtiter plate and printed at ambient temperature and relative humidity of 50-65%.
5. Glycan Microarray with “Map”	
Array layout	Each slide contains 3 replicate arrays, consisting of a 4x4 (16) subarray pattern with each subarray containing 12x18 features (not all features contain a printed sample).
Glycan identification and quality control	In-house sialoside array, consisting of 135 defined glycans (Supplementary Table 1). Quality control was assessed by incubation with plant lectins, AAL, ECA and SNA, to monitor fucosylations, de-sialylation and NeuAc-a(2-6) terminated glycans, respectively. Supplemental Experimental Procedures 2.Array Quality Control by Plant Lectins. Supplemental Figure S3 Peng et al., Glycobiology (2012) PMID: 22786570
6. Detector and Data Processing	
Scanning hardware	Innoscan 1100AL (Innopsys)

Scanner settings	Scanning resolution: 10 □m / pixel Laser channel: 532 PMT Voltages: Adjusted for each sample to achieve maximum signal without saturation of any single spot. Scan power: Adjusted for each sample to achieve maximum signal without saturation of any single spot.
Image analysis software	Mapix (Innopsys)
Data processing	Output .txt files containing calculated data were processed in MS Excel to determine the mean signal value of 6 replicate spots with highest and lowest signals removed (e.g. average of 4 spots).
7. Glycan Microarray Data Presentation	
Data presentation	The microarray binding results are in **Figure 2**. Binding results are presented as 2D bar graphs with bars representing averaged mean signal of each glycan and error bars representing standard deviation.
8. Interpretation and Conclusion from Microarray Data	
Data interpretation	No software or algorithms were used to interpret processed data.
Conclusions	During circulation in seals, the avian-origin A/H10N7 viruses acquired mutations that may have facilitated efficient virus spread in the new host and associated transmissibility in the ferret model. The attachment patterns of A/Puerto Rico/8/1934 (PR8) viruses harboring, H10sealNL, H10mall or mutant H10 HA proteins were characterized using the sialoside glycan array. We found that the changes required for infection of seals caused a decrease in the avidity of the virus for avian-type receptors and an increase in its preference for human-type receptors. The changes were caused by substitutions in the 220-loop that forms one edge of the receptor-binding pocket, in particular the amino acid substitution Q226L. This change also occurred in the HA of an aerosol or respiratory droplet-transmissible mutant of the initial avian influenza virus that infected seals; it was found when the initial virus replicated in ferrets, and it occurred in viruses isolated in the late phases of the outbreak presumably as a result of selection during the outbreak.

SUPPLEMENTAL FIGURES

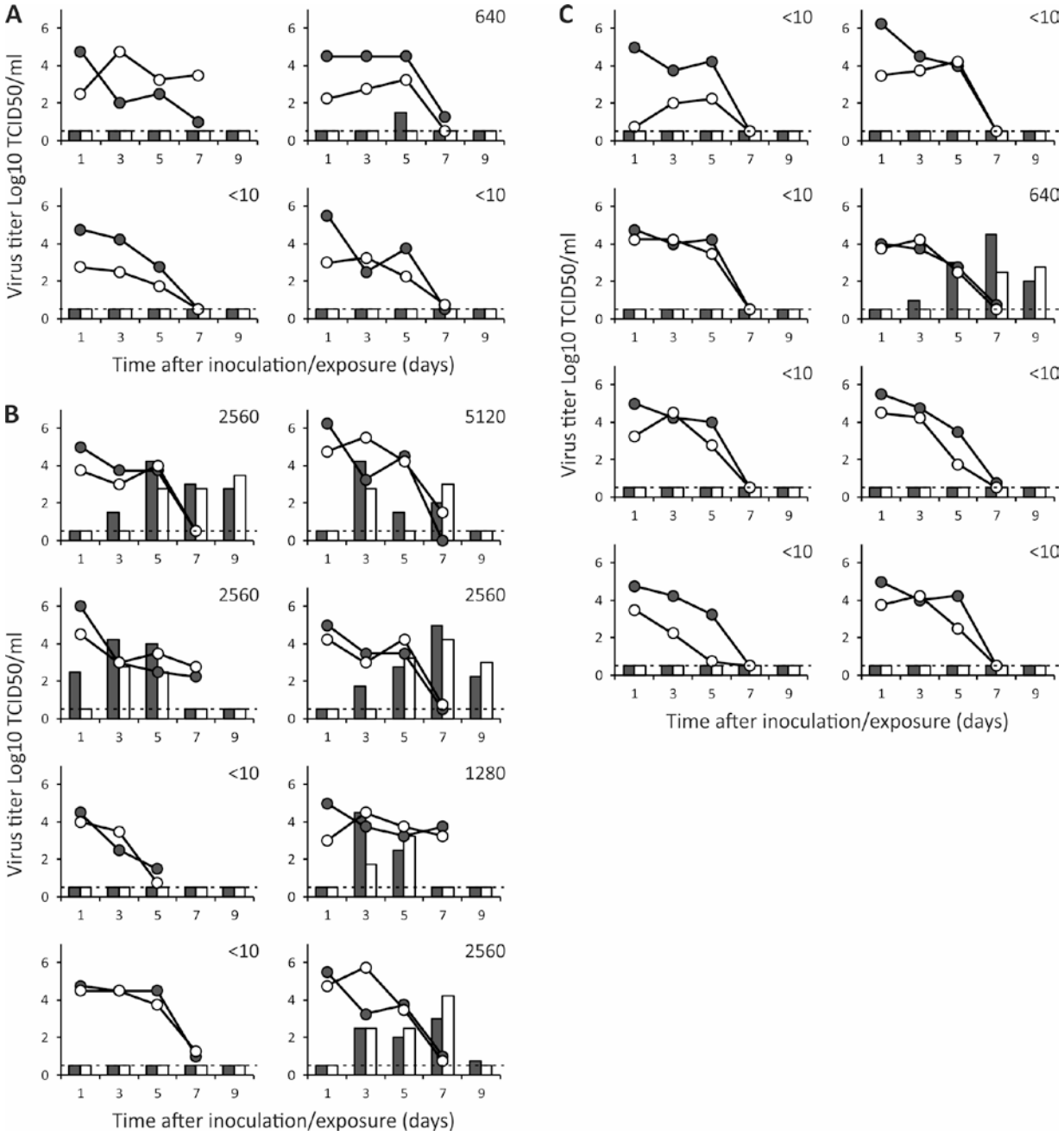

Figure S1. Related to Figure 1. Transmission of A/H10N7 viruses via aerosols or respiratory droplets between ferrets. Transmission experiments are shown for individual donor-recipient ferret pairs for (A) H10sealG, (B) H10sealNL and (C) H10mall. Donor ferrets were inoculated intranasally with 10^6 $TCID_{50}$ of virus and housed individually in transmission cages. A naïve recipient ferret was added to each transmission cage adjacent to a donor ferret at 1dpi. Virus titers in throat and nose swabs of donors (black and white lines respectively) and recipients (black and white bars respectively) were determined by end-point titration in MDCK cells. Aerosol or respiratory droplet transmission was observed in 1 out of 4 ferret pairs for H10sealG, 6 out of 8 ferrets pairs for H10sealNL and 1 out of 8 ferret pairs for H10mall. Numbers in each panel indicate the HI titer in serum collected from the recipient animal at 14 dpi. The lower limit of virus detection was <0.5 $Log_{10}TCID_{50}$/ml.

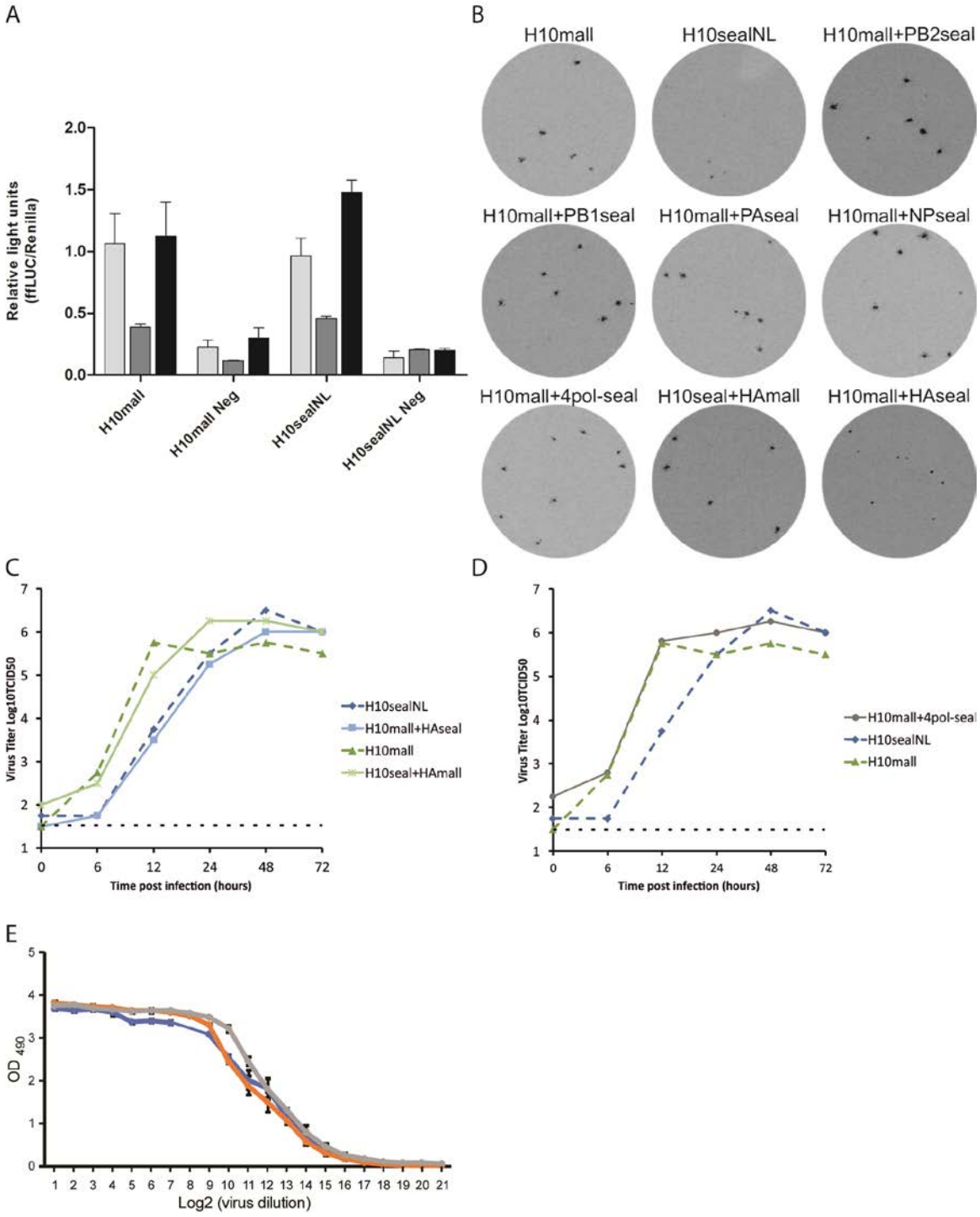

Figure S2. Related to Figure 1. (A) Minigenome reporter assay in 293T-cells. Plasmids encoding PB2, PB1, PA, and NP were cotransfected with a vRNA reporter encoding firefly luciferase. Luminescence of firefly luciferase was standardized using a plasmid constitutively expressing Renilla luciferase. Results are calculated as relative light units (firefly luciferase/ Renilla luciferase). Three independent experiments are shown (in light grey, dark grey and black). Error bars indicate the SD from the average of three independent experiments; Neg = NP plasmid was omitted. H10mall and H10sealNL had similar polymerase activity. (B) Plaque assay. MDCK cells were inoculated with H10mall, H10sealNL and H10mall/H10sealNL reassortants. After 40 hr, plaque formation was visualized by influenza NP-specific staining and digital images were created to compare plaque size. H10mall produced larger plaques than

H10sealNL. Reassortant H10mall viruses harboring either one or all four H10sealNL polymerase complex proteins displayed plaque sizes similar to H10mall, suggesting that the difference in plaque size between H10sealNL and H10mall was not due to the polymerase activity. (C and D) Replication kinetics in seal kidney cells. Seal kidney cells were inoculated with 0.1 $TCID_{50}$/cell of H10sealNL (diamonds), H10mall+HAsealNL (squares), H10mall (triangles), H10sealNL+HAmall (asterisks) or H10mall+4pol-sealNL (circles), and supernatant samples were harvested 6, 12, 24, 48 and 72 h later. Virus titers were determined in MDCK cells. Similar to the results from the plaque assay, viruses harboring the H10mall HA (H10mall and H10sealNL+HAmall) replicated faster than viruses harboring an H10sealNL HA (H10sealNL and H10mall+HAsealNL). Introduction of the four polymerase complex proteins PB2, PB1, PA and NP of H10sealNL into H10mall, did not change the replication kinetics of H10mall. (E) NA activity of H10N7 neuraminidases. NA activity of serially diluted H10mall (grey line), H10sealG (blue line) and H10sealNL (orange line) was measured by detecting desialylation of the highly glycosylated fetuin in the enzyme-linked lectin assay. The terminal galactoses that become exposed after desialylation is detected by PNA-HRPO. The intensity of the signal after addition of substrate depends on the level of desialylation and thus NA activity. The mallard N7 NA had slightly higher activity than the seal NA's. However the observed difference was only two-fold, which is within the error of the assay. Because of this small difference we concluded that the activities of the three different NA's were similar.

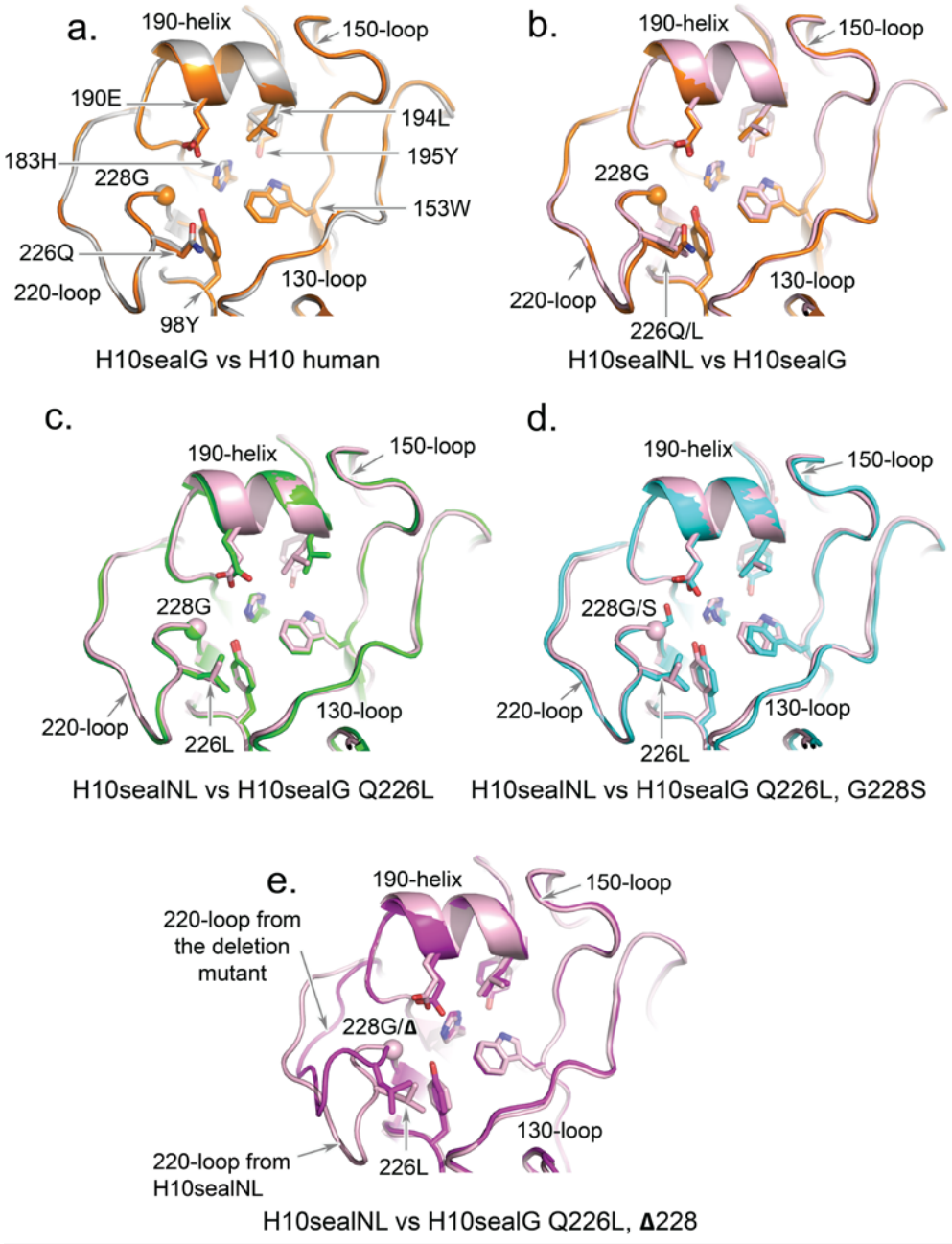

Figure S3. Related to Figure 4 and Figure 5. Comparison of A/H10 human HA, H10sealG, H10sealG Q226L,Δ228, H10sealG Q226L, H10sealG Q226L, G228S and H10sealNL. The figure shows that the orientations and positions of residues in H10sealG receptor binding site are similar to those of corresponding residues in the A/H10 human-type receptor binding site (a) (root-mean-square deviation (rmsd) Cα = 0.3 Å) and to H10seal NL (b), (rmsd Cα = 0.9 Å) by superposition. H10sealG Q226L (c), H10sealG Q226L, G228S (d) and H10sealG Q226L,Δ228 (e) receptor binding sites are superposed to H10sealNL receptor binding site respectively for comparison. The positions of the side chains of residue 226, 228, 190, 194, 195, 183, 153 and 98 in H10sealG are indicated and compared to their counterparts in A/H10 human and H10sealNL. These residues in H10sealG Q226L,Δ228, H10sealG Q226L, H10sealG Q226L, G228S are also compared to the residues in H10sealNL. The orientations and positions of residues in H10sealG Q226L and H10sealG Q226L, G228S receptor binding sites are similar to those of corresponding residues in the H10sealNL receptor binding site by superposition (rmsd Cα are 0.2 Å and 0.3 Å respectively). A/H10 human, H10sealG, H10sealNL, H10sealG Q226L,Δ228, H10sealG Q226L and H10sealG Q226L, G228S are colored in silver, orange, pink, magenta, green and cyan respectively.

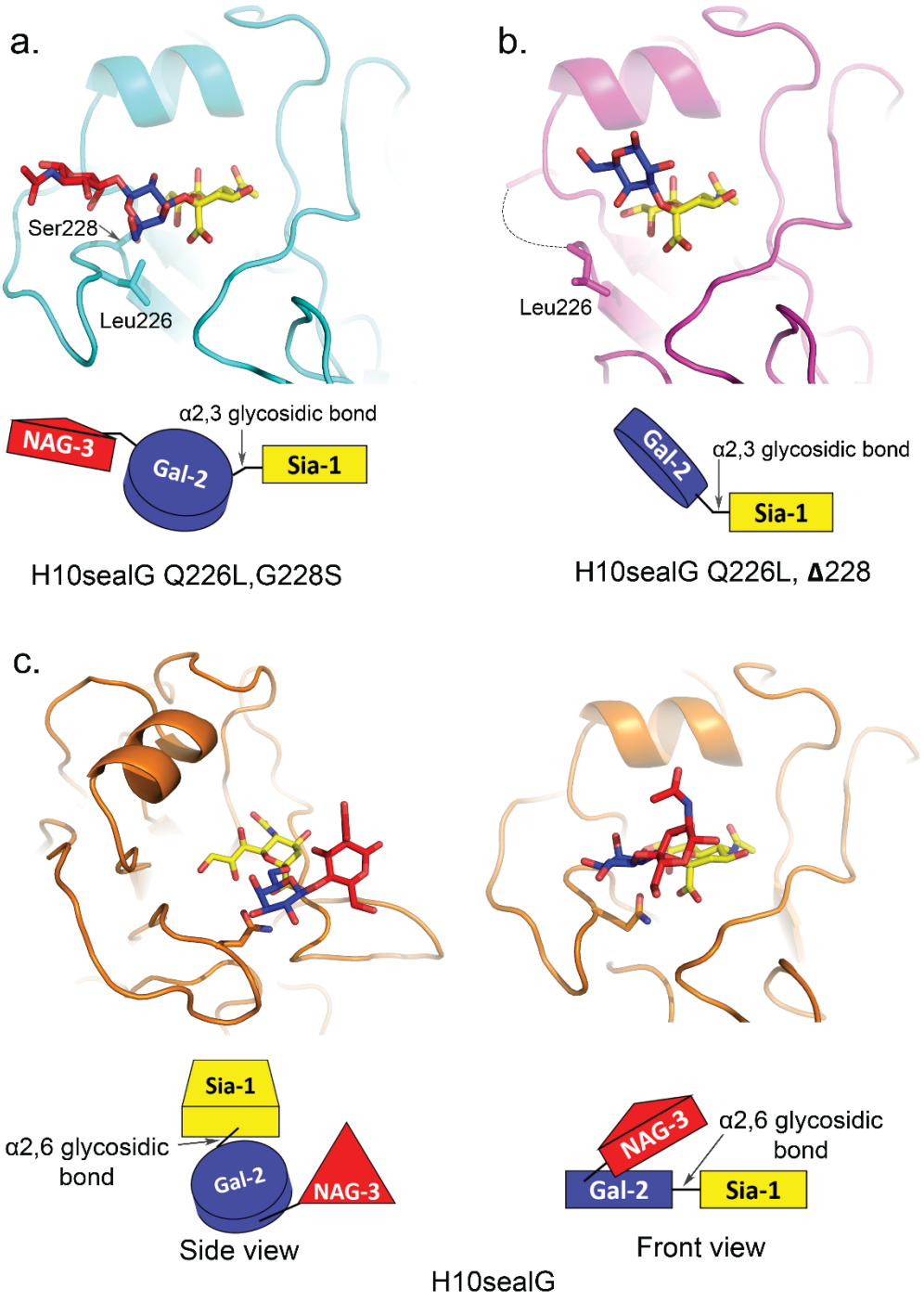

Figure S4. Related to Figure 4. Avian-type receptor binding features of H10sealG Q226L, G228S and H10sealG Q226L,Δ228 and human-type receptor binding features of H10sealG. The conformations of avian-type receptors bound to H10sealG Q226L, G228S and H10sealG Q226L,Δ228 and their schematic representations are shown in panel (a-b) respectively. The side and front views of the conformations of human-type receptors bound to H10sealG are shown in left and right sides of panel (c) respectively. The schematic representations of the receptor from the two views are also shown in panel (c). The sialic acid, galactose and N-acetylglucosamine of receptor analogue are coloured in yellow, blue and red individually. H10sealG Q226L, G228S is coloured in cyan in its complex structure (a) and H10sealG Q226L,Δ228 is coloured in magenta (b). H10sealG is coloured in orange in its complex structure (c). The 220 loop in H10sealG Q226L,Δ228 is disordered and the Cα of Leu-226 is repositioned (rmsd 2.2Å).

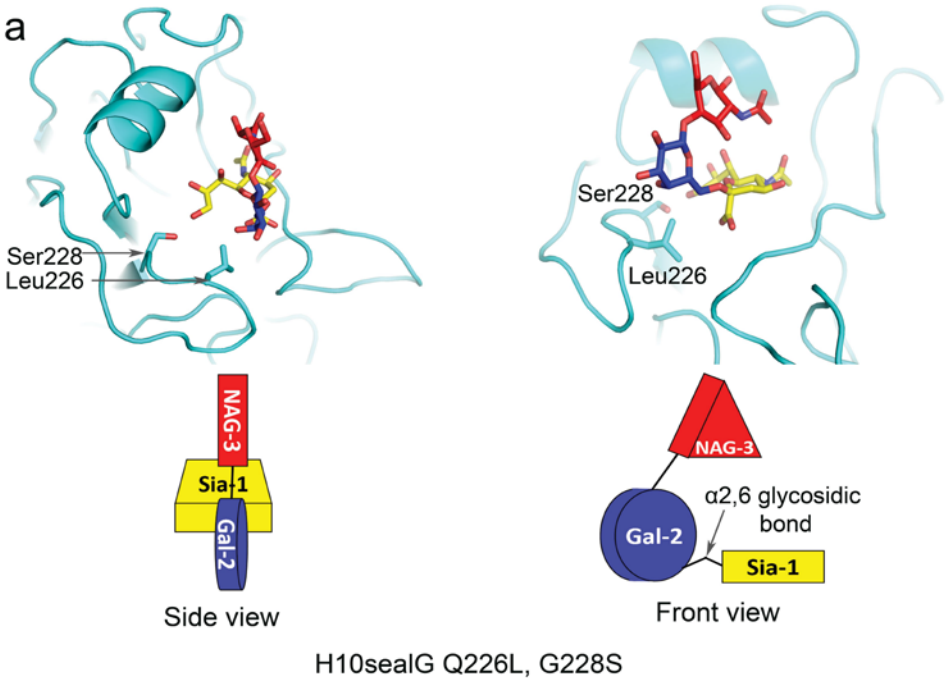

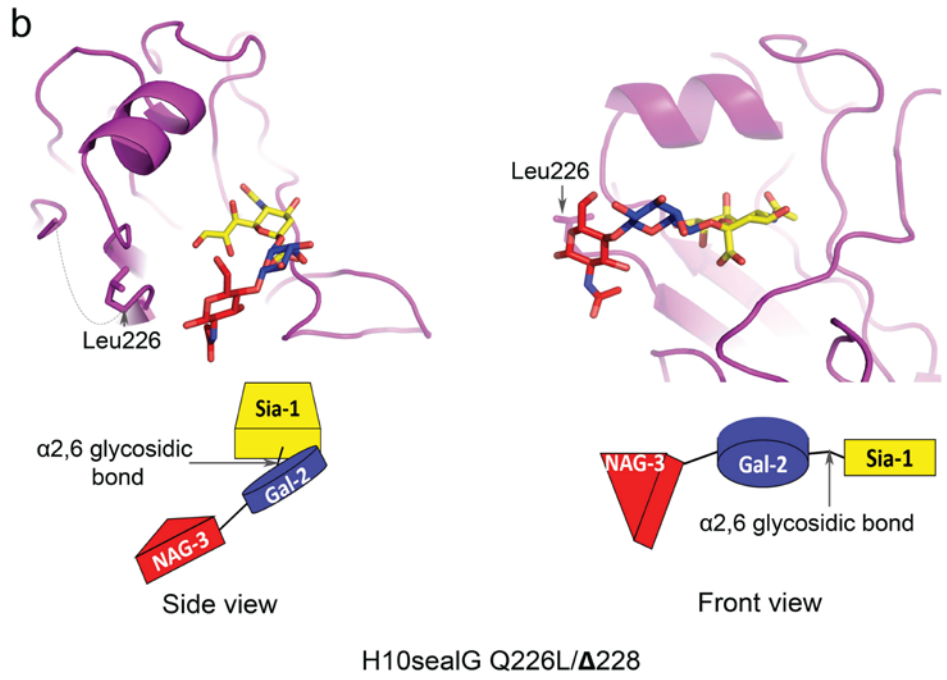

Figure S5. Related to Figure 5. Human-type receptor binding features of H10sealG Q226L, G228S and H10sealG Q226L,Δ228. The side and front views of the conformations of human-type receptors bound to H10sealG Q226L, G228S and H10sealG Q226L,Δ228 are shown in left and right sides of panel (a-b) respectively. The schematic representations of the conformations of the human-type receptors are shown in panel (a-b) as well. The sialic acid, galactose and N-acetylglucosamine of receptor analogue are coloured in yellow, blue and red individually. H10sealG Q226L, G228S is coloured in cyan in its complex structure (a). H10sealG Q226L,Δ228 is coloured in magenta (b).

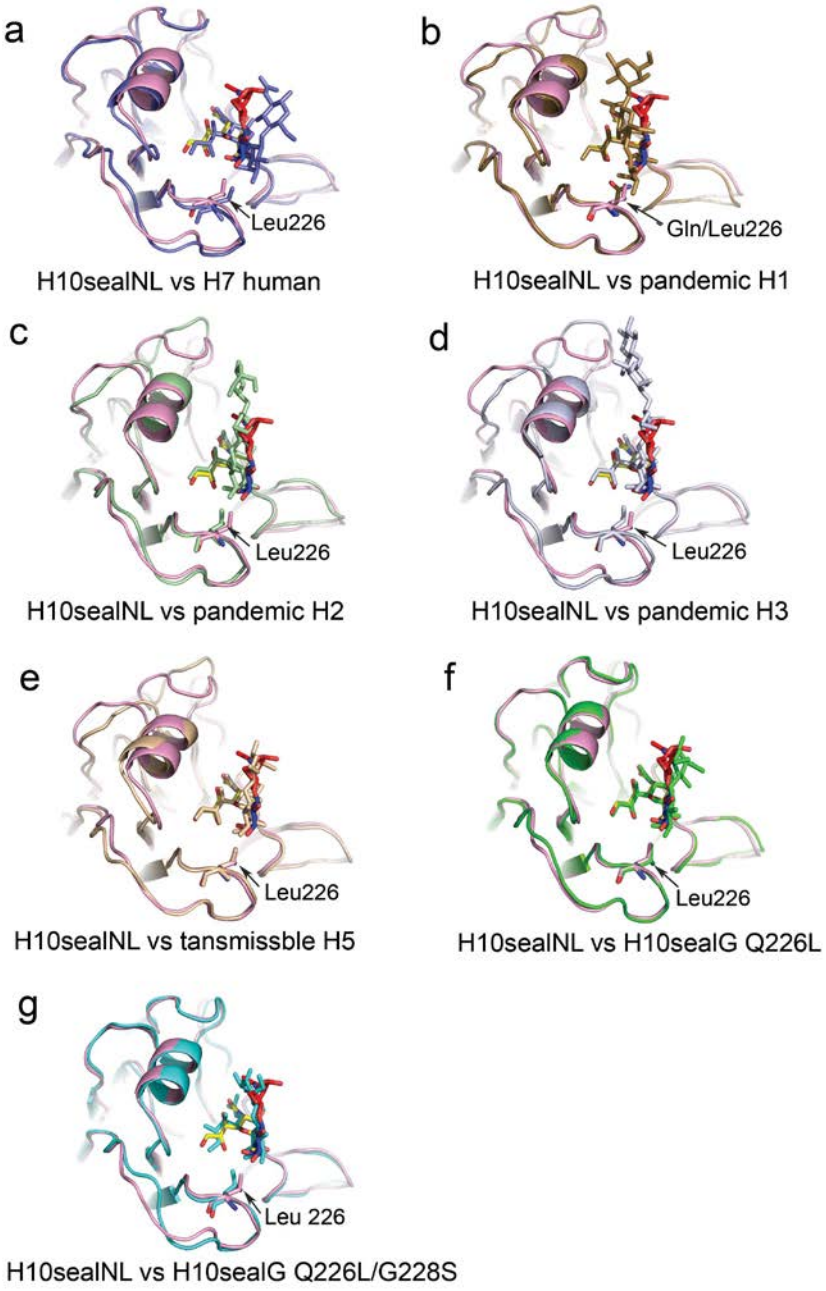

Figure S6. Related to Figure 5. Comparison of the conformation of human-type receptor bound to H10sealNL to that of human-type receptor bound to pandemic human HAs and H10sealG mutants. The figure shows the superposition of human-type receptor bound to H10sealNL to human-type receptors bound to human A/H7N9 (A/Anhui/1/2013) (a), pandemic A/H1 (b), pandemic A/H2 (c), pandemic A/H3 (d), transmissible A/H5N1 (A/Vietnam/1194/2004) (e), H10sealG Q226L (f) and H10sealG Q226L/G228S (Sia-1 slightly different; carboxylate group rmsd 1.4-2.4Å (g). A/H7 human is coloured in purple and pandemic A/H1 is coloured in brown. Pandemic A/H2 is coloured in light green and pandemic A/H3 is coloured in light purple. Transmissible A/H5 is coloured in beige and H10sealG Q226L is coloured in green. H10sealG Q226L/G228S is coloured in cyan and H10sealNL is coloured in pink. The sialic acid, the galactose and the N-acetylglucosamine of human-type receptor analogue in H10sealNL are coloured in yellow, blue and red respectively.

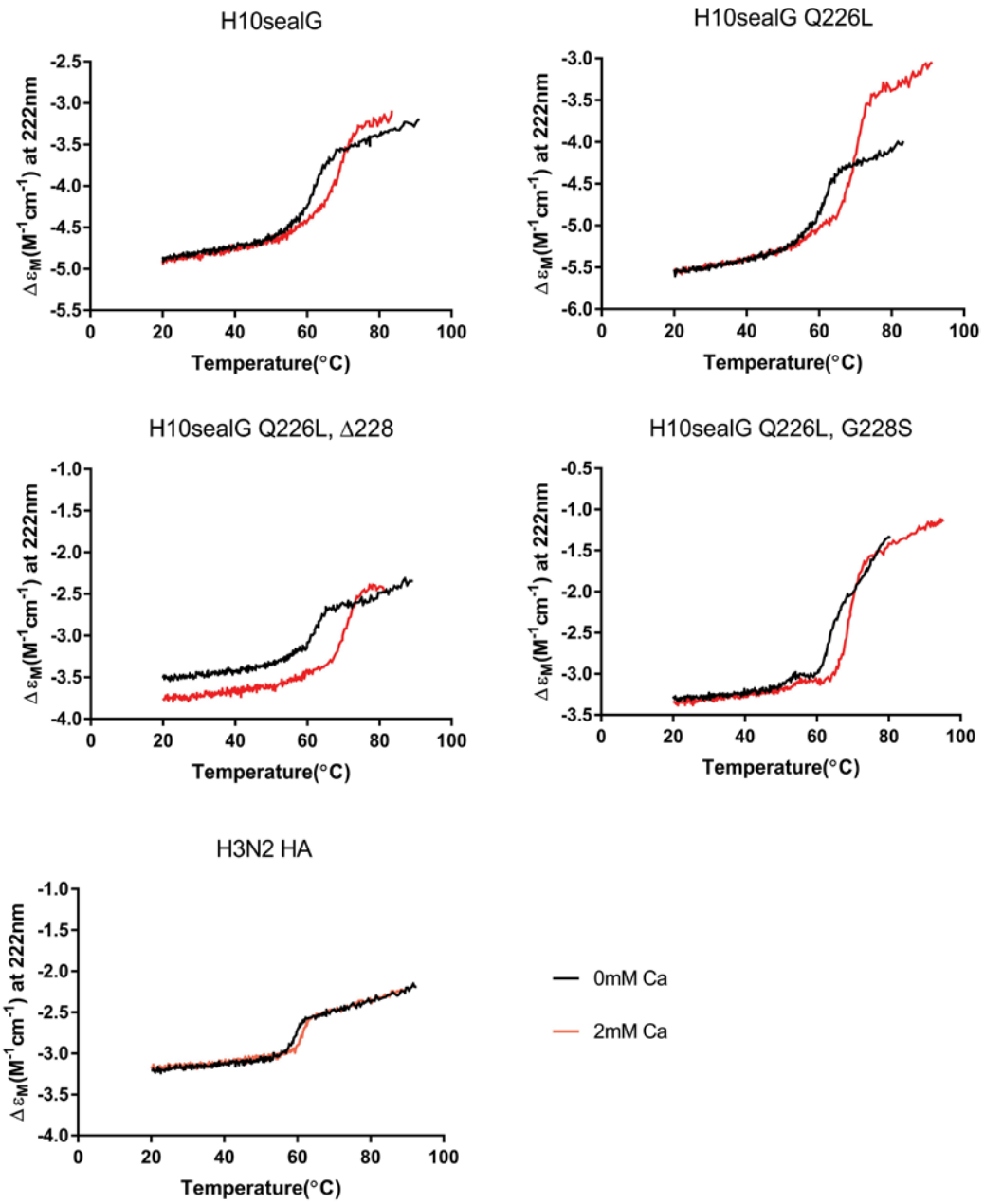

Figure S7. Related to Figure 6. The influence of calcium on thermal stability of A/H10seal HA, its variants and A/H3 HA. The unfolding curve in the presence of 2mM calcium is coloured in red while the unfolding curve in the absence of 2mM calcium is coloured in black.

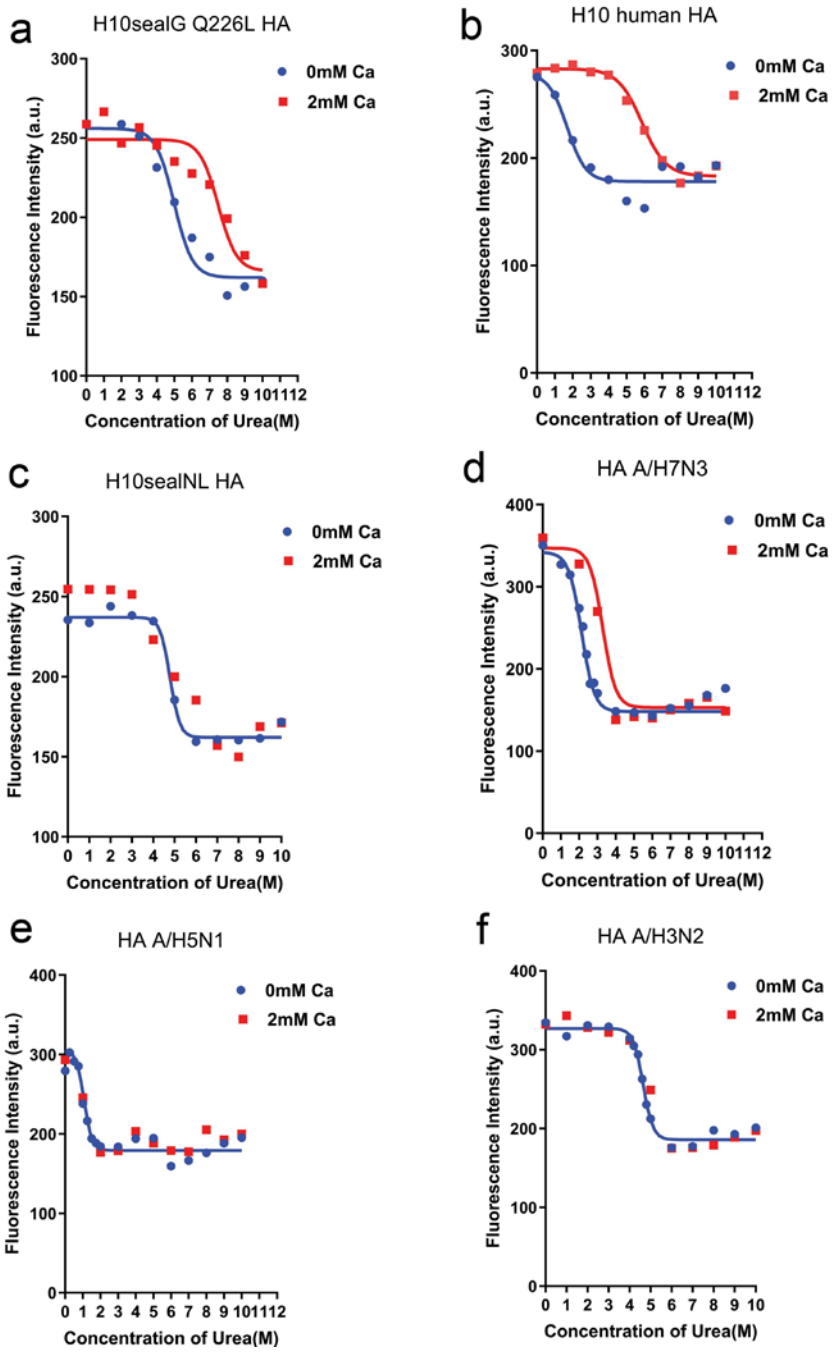

Figure S8. Related to Figure 6. The influence of calcium on the stability of A/H10, A/H7, A/H5 and A/H3 HA's. The tryptophan fluorescence signals of (a) H10sealG Q226L HA, (b) human A/H10 HA, (c) H10sealNL HA, (d) A/H7N3 (A/turkey/Italy/214845/2002) HA, (e) A/H5N1 (A/Vietnam/1194/2004) HA and (d) A/H3N2 (A/Aichi/2/1968) HA at 341nm are plotted against different concentrations of urea from panel a to f respectively. Data for HA in the absence of calcium are coloured in blue while data for HAs in the presence of 2mM calcium are coloured in red. The affinity of human A/H10N8 HA (A/Jiangxi-Donghu/346/2013) for calcium at room temperature was calculated to be 8.048 μM. The affinity of the H10sealG Q226L mutant for calcium at 30°C was 16 μM and the calculated affinity at room temperature was 5.6 μM, close to the affinity of A/H10 human HA. In contrast, the affinity of A/H7N3 HA (A/turkey/Italy/214845/2002) for calcium at room temperature was 75.12 μM, more than 10-fold lower than the affinity of H10sealG Q226L. Calcium did not bind to aerosol or respiratory droplet-transmissible H10sealNL, A/H3N2 (A/Aichi/2/1968) or A/H5N1 (A/Vietnam/1194/2004) HAs.

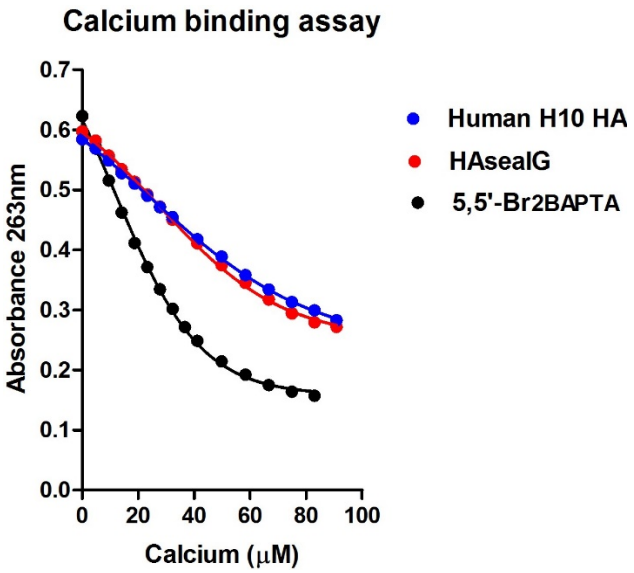

Figure S9. Related to Figure 6. Comparison of calcium binding by H10sealG human A/H10 HA. Calcium binding assays were performed by titrating the calcium chelator, 5, 5'-Br_2BAPTA with 1mM calcium. The absorbance of 5, 5'-Br_2BAPTA in the presence of human A/H10 HA or H10sealG HA or in buffer are plotted against the concentration of calcium. The calcium binding curve for human A/H10 HA is coloured in blue, that for H10sealG is coloured in red, and that for 5'-Br_2BAPTA is coloured in black and taken as a control. Data for the H10sealG HA was analysable using a model with three stoichiometric association constants: $K_1 = 1.4 \pm 0.25 \times 10^6\ M^{-1}$, $K_2 = 4.2 \pm 0.9 \times 10^5\ M^{-1}$, and $K_3 = 8.5 \pm 2.8 \times 10^4\ M^{-1}$. A protein with three identical non-interacting sites with an intrinsic association constant (k) would be expected to have stoichiometric association constants in the following pattern: $K_1 = 3k$, $K_2 = k$, and $K_3 = k/3$. This is very close to the pattern observed for the HAsealG and therefore it was concluded that this HA trimer contains three identical non-interacting calcium binding sites with an affinity of approximately 2.3 μM. Similar experiments with the human A/H10 HA from A/Jiangxi-Donghu/346/2013 (A/H10N8) were also consistent with this trimer containing three identical non-interacting calcium binding sites, in this case with an affinity of approximately 2.9 μM.

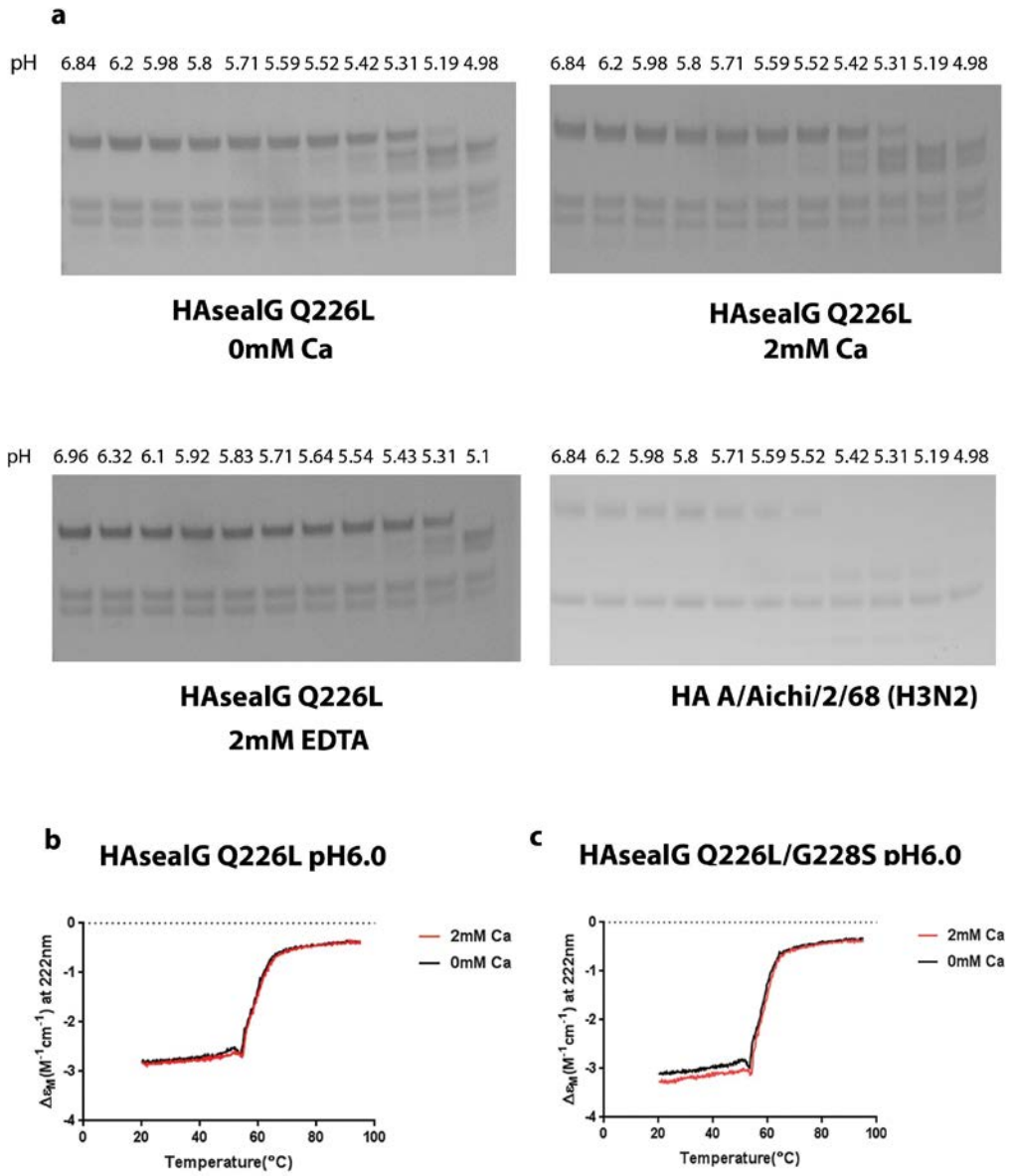

Figure S10. Related to Figure 6. The influence of calcium on the stability of A/H10 seal HAs. The trypsin susceptibilities of H10sealG Q226L mutant from pH 6.8 to 5.0 in the presence or the absence of 2mM calcium or in the presence of EDTA are shown in panel a and the data for A/H3 HA are presented as a control. The CD signal of H10sealG Q226L mutant and of H10sealG Q226L/G228S mutant at 222nm are plotted against temperature and shown in panel b and c respectively. The thermal unfolding curves of A/H10 seal HAs in the presence and the absence of 2mM calcium are shown in red and black individually.